eLife

Reviewed Preprint
v2 • August 22, 2024
Revised by authors

Reviewed Preprint
v1 • April 16, 2024

Neuroscience

Associative plasticity of granule cell inputs to cerebellar Purkinje cells

Rossella Conti, Céline Auger

Université Paris Cité, CNRS, Saints-Pères Paris Institute for the Neurosciences, Paris, France

Abstract

Granule cells of the cerebellum make up to 175 000 excitatory synapses on a single Purkinje cell, encoding the wide variety of information from the mossy fibre inputs into the cerebellar cortex. The granule cell axon is made of an ascending portion and a long parallel fibre extending at right angles, an architecture suggesting that synapses formed by the two segments of the axon could encode different information. There are controversial indications that ascending axon (AA) and parallel fibre (PF) synapse properties and modalities of plasticity are different. We tested the hypothesis that AA and PF synapses encode different information, and that association of these distinct inputs to Purkinje cells might be relevant to the circuit and trigger plasticity, similarly to the coincident activation of PF and climbing fibre inputs. Here, by recording synaptic currents in Purkinje cells from either proximal or distal granule cells (mostly AA and PF synapses respectively), we describe a new form of associative plasticity between these two distinct granule cell inputs. We show for the first time that synchronous AA and PF repetitive train stimulation, with inhibition intact, triggers long term potentiation (LTP) at AA synapses specifically. Furthermore, the timing of presentation of the two inputs controls the outcome of plasticity and induction requires NMDAR and mGluR1 activation. The long length of the PFs allows us to preferentially activate the two inputs independently, and despite a lack of morphological reconstruction of the connections, these observations reinforce the suggestion that AA and PF synapses have different coding capabilities and plasticity that is associative, enabling effective association of information transmitted via granule cells.

eLife assessment

This study presents **valuable** findings on an unresolved question of cerebellar physiology: Do synapses between Purkinje cells and granule cells, made by the ascending part of the granule cells' axon, have different properties than those made by parallel fibers? The authors conducted patch-clamp recordings on rat cerebellar slices and found a new type of plasticity in the synapses of the ascending part of granule cell axons. The experiments are well-designed with appropriate controls, and the study provides **solid** evidence for the new form of cerebellar synaptic plasticity.

https://doi.org/10.7554/eLife.96140.2.sa4

Introduction

The ability to discriminate self generated from external stimuli is essential to apprehend the world as movement itself activates sensory receptors. In fish, discrimination of self from external stimuli has been shown to rely on associating motor command and sensory feedback in cerebellar-like structures (Montgomery & Bodznick, 1994; Sawtell, 2017). This is achieved by modifying the motor inputs to generate a negative image of the associated sensory inputs, effectively subtracting the predictable sensory inputs. This way, only unpredicted inputs are output by the principal cells. While in most cases the role of the cerebellum in sensory information processing is still unclear, theoretical models and work on plasticity suggest that it might similarly be involved in cancellation of predictable sensory inputs, but distinct sensory and motor synapses have yet to be identified in the cerebellum. The role of the cerebellum in motor learning and coordination has been well documented, but it is now clear that it is also involved in a number of higher cognitive functions (Schmahmann & Sherman, 1998; Stoodley & Schmahmann, 2010). An intriguing possibility, in the wider context of the cerebellum, is that receptive field and contextual inputs are encoded differentially by the granule cell AA and PF synapses. These inputs might be functionally associated based on relative timing to subtract predictable inputs, and output only unpredicted inputs, as observed for motor and sensory inputs in cerebellar-like structures.

Sensorimotor information is delivered to the cerebellar cortex by mossy fibres and relayed by granule cells (GCs) to the Purkinje cells (PCs) and inhibitory network for integration. Anatomically, the axon of a GC first extends through the PC layer and into the molecular layer, making up the ascending portion of the axon (AA), then bifurcates at a right angle, forming a PF that extends several millimetres along the folium in both directions. As a consequence, an AA can form multiple synapses with a few overlaying PCs in the same sagittal plane as the GC soma, distributing information to a restricted number of cells, whereas PFs course through the dendritic trees of hundreds of PCs along the lobule (Napper & Harvey, 1988), distributing information widely to other microzones. This morphology and functional data have suggested that PC activity might be principally driven by local GCs via AA synapses (Cohen & Yarom, 1998), while distant GCs might modulate its activity via the PF system to provide the PC with less specific contextual information.

In the adult rat, an estimated 175k excitatory PF synapses encode information on the dendritic tree of a single PC (Napper & Harvey, 1988). We previously identified two PF synaptic populations with different molecular signatures (Devi et al., 2016). However, PF synapses have usually been treated as a uniform population, and we know little about the way the variety of information received by PCs is encoded at synaptic level. Isope and Barbour (Isope & Barbour, 2002) estimated that 85% of PF synapses are silent, as suggested by in vivo data (Ekerot & Jörntell, 2001), however that proportion was significantly lower for local GCs and presumably AA synapses. In this study and that by Walter (Walter et al., 2009), properties of AA synapses were found to be indistinguishable from PF synapses. On the other hand, a study by Sims and Hartell (2005), has shown that AA and PF synaptic properties and susceptibility to plasticity are different. AA synapses were shown to be refractory to plasticity with well described protocols. Neither associative CF-mediated long term depression (LTD) nor LTP could be induced (Sims & Hartell, 2005; Sims & Hartell, 2006). These observations, together with the anatomical properties of the GC axon, suggest that AA and PF synapses can transmit different types of information and play different roles in cerebellar computation.

In this study we asked whether coincident activation of synapses formed by proximal and distal GCs (mostly AA and PF synapses respectively) might trigger specific synaptic plasticity of GC inputs. We show that a protocol pairing stimulation of AAs and PFs, with inhibition preserved, results in LTP of the AA inputs, while PF inputs are depressed although not significantly. AA-LTP is

timing-dependent and relies on NMDAR and mGluR1 activation, bringing together these two pathways. $GABA_AR$ activation was also required for efficient induction and maintenance of plasticity. Finally we show that the different plasticity found for AA and PF inputs is not merely due to the differential spatial distribution of their synapses on the dendritic tree.

Results

Associative plasticity of AA synapses

To test for associative plasticity between ascending axon and parallel fibre inputs we positioned two separate stimulating electrodes to achieve activation of different GC inputs onto a recorded PC (**Fig. 1A** top panel). To stimulate PFs, a stimulation pipette was positioned in the molecular layer, 100 to 200 µm away from the dendritic tree of the recorded cell. The average length of a PF is between 4.2 and 4.7 mm (Pichitpornchai et al., 1994). If we assume that only granule cells located within the 50 µm thick layer of the PC dendritic tree can make AA synapses, and take the average length of a parallel fibre, they represent only 1 to 2 % of granule cells or parallel fibres. Therefore the vast majority of fibres stimulated locally in the molecular layer belong to GCs distant from the recorded cell and only 1 to 2% are likely to originate from that 50 µm layer and make AA synapses. To stimulate AAs, a second stimulation pipette was positioned in the GC layer, within a narrow window centred on the PC somato-dendritic plane. The GCs stimulated in this position have a high probability of making AA synapses onto the dendritic tree of the PC, although a small proportion could also make synapses from the proximal portion of PFs after bifurcation. For the sake of simplicity, we will use the terms AA and PF synapses thereafter although the terms proximal and distal synapses (with respect to GC soma) might be more appropriate.

The EPSC amplitude of AA and PF pathways were sampled with a pair of stimulations each (**Fig 1A** middle panel). On average, the amplitude of the AA-EPSC during baseline recordings was 110 ±12 pA (median 90 pA) and PF-EPSC 480 ±100 pA (median 288 pA, n = 25), and the paired pulse ratio (PPR) was PPR_{AA} 1.93 ±0.08 and PPR_{PF} 1.89 ±0.07. Inhibitory inputs were preserved, and EPSCs were often followed by outward IPSCs. After baseline recording, a protocol aimed at inducing plasticity was applied (synchronous stimulation of both inputs by a train of 15 pulses at 100 Hz, every 3 s, 100 times, in Current clamp, see **Fig. 1A** bottom panel). Test of the AA and PF amplitude was then resumed. **Figure 1A** middle panel shows a sample experiment with average traces of the AA-PSC, in blue, and the PF-PSC, in orange, 5 min before (continuous line) the plasticity induction protocol, and 25-30 min after the protocol (dotted line). Subtraction traces (25-30 min - last 5 min) are shown in grey to highlight changes. The AA-EPSC amplitude is increased while the PF-EPSC amplitude is decreased. **Figure 1B** top panel shows the time course of 24 such experiments for the AA pathway and 25 for the PF pathway with amplitude normalised to the last 5 minutes of control before plasticity induction. It shows that on average, following the induction protocol, we observed a long term change of opposite sign of the two inputs. The AA peak EPSC amplitude increased to 162 ±15% of baseline immediately after the induction protocol and then slowly decayed within 15 mins to stabilise at a value of 131 ± 7 % 25 to 30 minutes after induction, significantly larger than the baseline (p=7e-5 one-tailed T-test, n=24). The PF-EPSC on the other hand was almost unchanged immediately after the protocol (91 ±9%) and decreased to 65 ±5 % of baseline at 25-30 min, significantly smaller than the baseline (p=1e-7 one-tailed T-test, n=25).

Figure 1B also reveals a rundown of the EPSC amplitude during the baseline period, potentially obscuring long term changes induced by plasticity. A series of control experiments was conducted to quantify the rundown (No Stim experiments, see supplementary Figure 1). After the baseline period, recording was switched to Iclamp for 5 min, but no stimulation was delivered during that period. Continuous lines **Figure 1B** top panel show the average time course for 17 No Stim experiments for the AA- (blue) and PF-EPSCs (orange). On average, 25 to 30 minutes after the Iclamp period, the AA-EPSC was 80 ± 6% of baseline (n= 16, significantly smaller than baseline p =

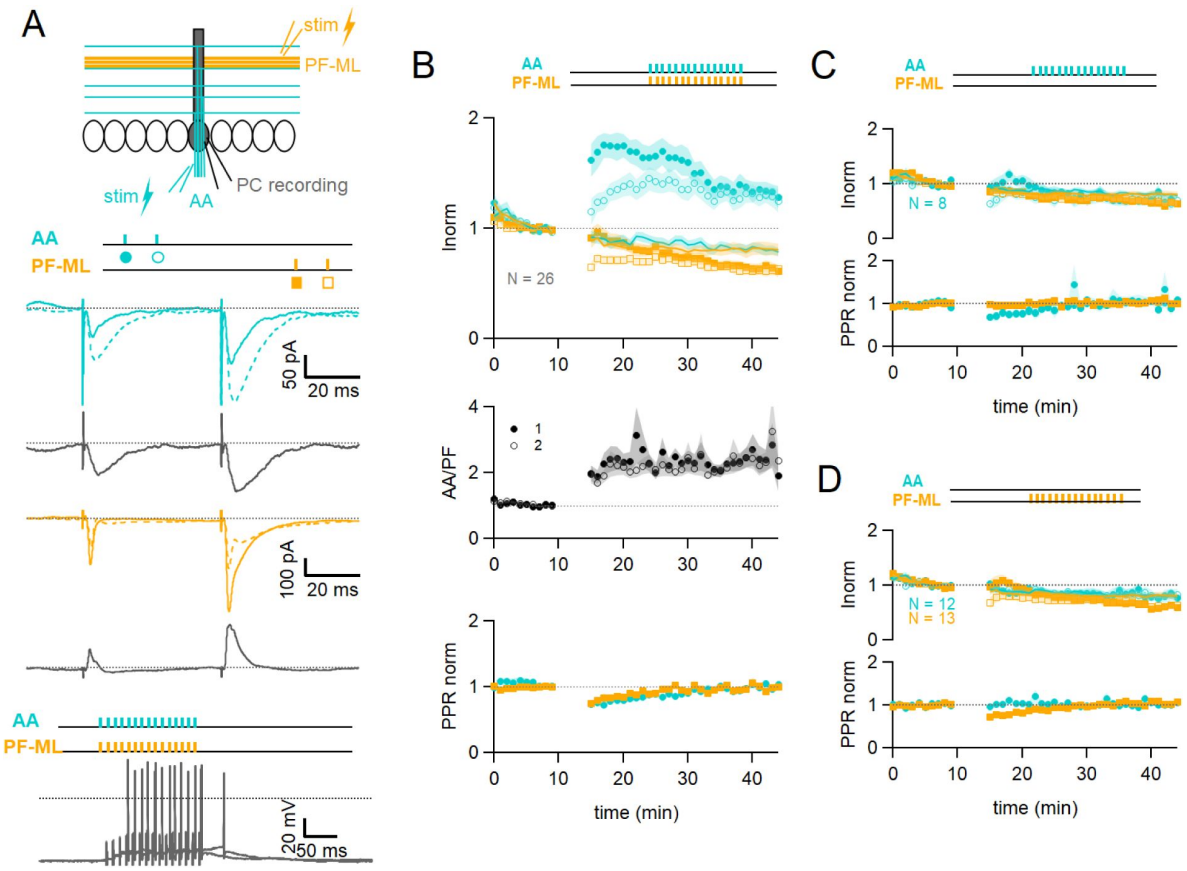

Figure 1

Associative plasticity of AA and PF inputs.

A, top. Whole cell recording in a PC. Two stimulation electrodes are used to activate GC inputs: one in the molecular layer to stimulate PFs (orange), and one in the GC layer to stimulate AAs (blue). The test stimulation protocol is depicted with colors and symbols as used in the plots in the following sections for the first (closed) and the second EPSCs (open). **Middle**, AA- and PF-PSCs sampled with a pair of pulses (dt = 50 ms), every 10 s. Traces from one experiment: average AA-PSC (blue) and PF-PSC (orange), before (5-10 min, continuous line) and after the induction protocol (25-30 min, dotted line). Subtraction in grey. AA-EPSC amplitude increased while PF-EPSC amplitude decreased. No antagonist was applied. Evoked responses consisted of an EPSC often followed by an IPSC. **Bottom**, induction protocol. Recording switched to current clamp, V_H = -65 mV. AAs and PFs are stimulated synchronously by a train of 15 pulses at 100 Hz every 3 s for 5 min. Grey traces, responses to the first two trains of stimulation. **B Top**, plot of the average AA- and PF-EPSC amplitude normalised to baseline for synchronous stimulation (5-10min, n = 25, colours and symbols as in A) and control No Stim experiments (continuous lines). Following induction, a long term change of the inputs was observed. The amplitude of the AA-EPSC increased to 131% ± 7 % (N = 24) of baseline 25-30 min after induction. The PF-EPSC on the other hand decreased slowly to 65% ±5 % (N = 25) of baseline. Continuous lines show the average time course of AA- and PF-EPSC amplitudes during control No Stim experiments where no stimulation was performed during the Iclamp period (N = 17, see supplementary Figure 1), showing the extent of EPSC rundown during the course of the recordings. **Middle**, the average ratio of the normalised amplitudes of AA- and PF-EPSCs (AA/PF), highlighting the relative change of the inputs, doubles. **Bottom**, the average normalised paired pulse ratio (AA2/AA1 and PF2/PF1) is transiently decreased following induction. **C.** Average of 8 experiments with stimulation of the AA pathway only during induction (labels, colours and symbols as in A), and No Stim experiments overlaid (continuous lines). **Top**, the normalised amplitudes of AA- and PF-EPSCs progressively decreased to 72 % ± 7% (N = 8) and 64 % ± 6% (N = 8) of baseline respectively, not significantly different from No Stim experiments. Stimulation of the AA pathway alone is not sufficient to trigger AA-LTP. **D.** Average of 13 experiments with stimulation of the PF pathway only during induction (labels), and No Stim experiments overlaid (continuous lines). **Top**, the normalised AA-EPSCs showed a small and steady depression (84% ± 7 % of baseline after 25-30 min) whereas the PF-EPSC depressed over time (64% ± 6 %), not significantly different from No Stim experiments. Stimulation of the PF pathway on its own is not sufficient to trigger plasticity. **C** and **D bottom**, the PPR of the AA and PF pathways transiently decreased only for the pathway stimulated during induction. Values given are mean ± SEM. SEM represented by shading.

0.0004, and significantly smaller than synchronous stimulation protocol p = 10e-7) and the PF-EPSC was 81 ± 8% of baseline (N = 17, not significantly smaller than baseline p = 0.062, and not significantly larger than synchronous stimulation protocol p = 0.106), indicating a rundown of the amplitude for both pathways during experimental time, independent of the induction protocol. The extent of AA- and PF-EPSC rundown was not significantly different (n= 16 and 17 respectively, p = 0.82). These values can be used to correct long term changes. When compensating for rundown, the plasticity protocol caused a long lasting effective increase of the AA-EPSC to 164% of baseline and a decrease of the PF-EPSC to 80% of baseline on average.

Fig 1B middle panel shows the ratio of normalised AA and PF peak amplitudes (AA/PF). This measure highlights the relative amplitude change of AA and PF inputs, or relative plasticity, and eliminates changes common to both pathways, such as the rundown of synaptic responses. On average the normalised amplitude of the AA-EPSC more than doubles compared to that of the PF-EPSC, due to both the increase of the AA peak amplitude and the concomitant decrease of the PF, and this is sustained (AA/PF = 2.5 ± 0.4 with N = 24, p=3e-4 after 25-30 mins of induction). **Figure 1B** bottom panel shows the paired pulse ratio of normalised amplitudes (PPR) for both pathways. While the peak amplitude of the first response in the pair of stimulations showed a progressive decrease, the peak amplitude of the second response of both AA and PF underwent either potentiation or depression respectively, and was relatively stable thereafter. As a result, the normalised PPRs is transiently decreased following induction, but returns to its original value within 25-30 minutes (PPR_{AA} 1.03 ± 0.03, PPR_{PF} 0.99 ± 0.03, N= 24, p = 0.81). Changes of the PPR have been linked to a change of the presynaptic release probability (Zucker and Regehr, 2002). This suggests a transient presynaptic effect on release probability following induction and likely explains the progressive effects on AA and PF responses, but there was no significant long term change of the PPR, suggesting that the long term effects observed are linked to postsynaptic changes.

Additionally, the level of plasticity measured in a given input pathway did not depend on the amplitude of the synaptic response of that input nor on the sum of the amplitudes of the two pathways (see Supplementary Fig. 2B), showing that even relatively small inputs can trigger plasticity. We analysed the average number of spikes and the time to the first spike during the first 5 trains of stimulation of the induction protocol. All cells except one did spike, even those with relatively weak synaptic currents for the first evoked response. The plastic change for the AA-EPSC only slightly correlated with the number of spikes (Pr = 0.48) and the time to the first spike (Pr = 0.4), and no correlation was observed for PFs (see Supplementary Fig. 2C).

To test whether the plasticity observed is due to the co-activation of AA and PF inputs or the specific properties of the stimulated inputs, we performed a series of experiments in which only one of the pathways was stimulated during the induction protocol. **Figure 1C** depicts the average behaviour in 8 experiments where only the AA pathway was stimulated during induction. The average amplitude of the AA-EPSC progressively decreased to 72 % ± 7% (N = 8) of control 25-30 minutes after the protocol, similarly to the PF-EPSC (64 % ± 6% of control, N = 8), not different from No Stim experiments (p = 0.49 and p= 0.48 respectively). The normalised amplitude of the AA-EPSC was not significantly different from that of the PF-EPSC following induction (AA/PF: 1.2 ± 0.2 after 25-30 min, p =0.58, N = 8, **Fig. 1C** bottom panel). This shows that stimulation of the AA pathway alone is not sufficient to trigger AA-LTP. **Figure 1D** shows the average time course of 13 experiments where only the PF pathway was stimulated during induction. In this case, the AA pathway showed a decrease (84% ± 7 % of baseline after 25-30 min, N = 12), whereas the PF pathway developed a larger depression over time (64% ± 6 % of baseline), but not different from No Stim experiments (p = 0.63 and p = 0.25 respectively). The relative amplitude of the normalised AA-EPSC (AA/PF) increased slowly after induction and was significant after 25-30 min (AA/PF = 140%± 11 % of baseline, N = 12, p = 0.01), in line with the progressive depression of the PF

pathway. In these experiments, the PPR of the AA and PF pathways were transiently modified after induction, as in control, but only for the pathway stimulated during the protocol (see **Fig. 1C** and **1D** bottom panel).

Individual and average data are also presented **Figure 2C** for control, No Stim and AA and PF stimulation only for comparison. Stimulation of either pathway independently did not induce AA-LTP, showing that co-activation of AA and PF inputs is necessary, and AA-LTP is associative. The PF-EPSC decreased following the induction protocol but this was not significantly different from control No Stim experiments.

Timing dependence of plasticity

The relative timing of inputs might be relevant to functional association, as observed for CF-mediated LTD (Safo & Regehr, 2008). We tested whether the relative timing of stimulation of the AA and PF pathways affects plasticity. During the induction protocol, the AA input was stimulated 150 ms after or 150 ms before the PF input. **Figure 2A** shows that when stimulating AAs 150 ms after PFs, the amplitude of the AA- and PF-EPSCs was depressed to a similar extent (AA was 53 % ± 15 % and PF 50 % ± 20 % of baseline, n = 8, not significantly different from each other p = 0.84), transforming AA-LTP into LTD. These changes were significantly different from experiments with synchronous stimulation (p = 8e-5 for AA and p = 0.022 for PF). The relative amplitude of the AA to PF pathway increased but not significantly (AA/PF was 224 % ± 75 % of baseline, n = 8, p = 0.2). On the other hand, when stimulating AAs 150 ms before PFs (see **Fig. 2B**), the amplitude of the AA-EPSC was first facilitated and declined back to baseline (AA after 25-30 min was 97% ± 26%, n = 7, significantly smaller than synchronous stimulation p = 0.011), and the amplitude of the PF-EPSC was now close to baseline (84 % ± 12 %, n= 7, not significantly larger than synchronous stimulation, p = 0.062). The relative amplitude of the AA to PF pathway was not facilitated significantly (AA/PF was 126 % ± 31 % of baseline, p = 0.35), while the PPR slightly increased (PPR_{AA} = 114 % ± 6 %, p = 0.008, and PPR_{PF} = 107 % ± 5%, N = 7 and p = 0.09 respectively).

In summary (**Figure 2C**), following the induction protocol the AA-EPSC was 131% ± 7% (N = 24) of baseline when AA and PF stimulation was synchronous; it was 53% ± 15% when AA stimulation was given 150 ms after PF stimulation (N = 8), and 97 % ± 26 % (N = 7) when the PF stimulation was started 150 ms after AA stimulation. The PF-EPSC was 65 % ± 5 % of baseline (N = 25, significantly different from AA, p = $6e^{-11}$) when stimulation was synchronous, 50% ± 20% when AA stimulation was delayed by 150 ms (N = 8), and 84 % ± 12 % when PF stimulation was delayed by 150 ms (N = 7).

These experiments show that the relative timing of the AA and PF input stimulation determines the extent of plasticity of both GC synapses, sometimes in opposite directions. The AA-EPSC was either facilitated or depressed significantly when stimulation was synchronous or delayed with respect to PF-EPSC during the induction protocol.

Plasticity induction mechanism

PF-LTD and LTP have been linked to mGluR1 (Daniel et al., 1992; Konnerth et al., 1992; Hémart et al., 1995) and/or NMDAR activation (Casado et al., 2002; Bidoret et al., 2009; Bouvier et al., 2016; Kono et al., 2019), and KOs of either receptor show defects in cerebellar learning (Aiba et al., 1994; Nakao et al., 2019; Kono et al., 2019; Schonewille et al., 2021). mGluR1s are highly expressed by PCs and located postsynaptically at GC to PC synapses. mGluR1s activation requires PF train stimulation, and it has not been observed when stimulating sparse GC synapses (Marcaggi & Attwell, 2005). NMDARs on the other hand are expressed by molecular layer interneurons (Glitsch & Marty, 1999; Duguid & Smart, 2004) and GCs (Bidoret et al., 2009; Bidoret et al., 2015), where they are located on dendrites and presynaptic varicosities. NMDAR

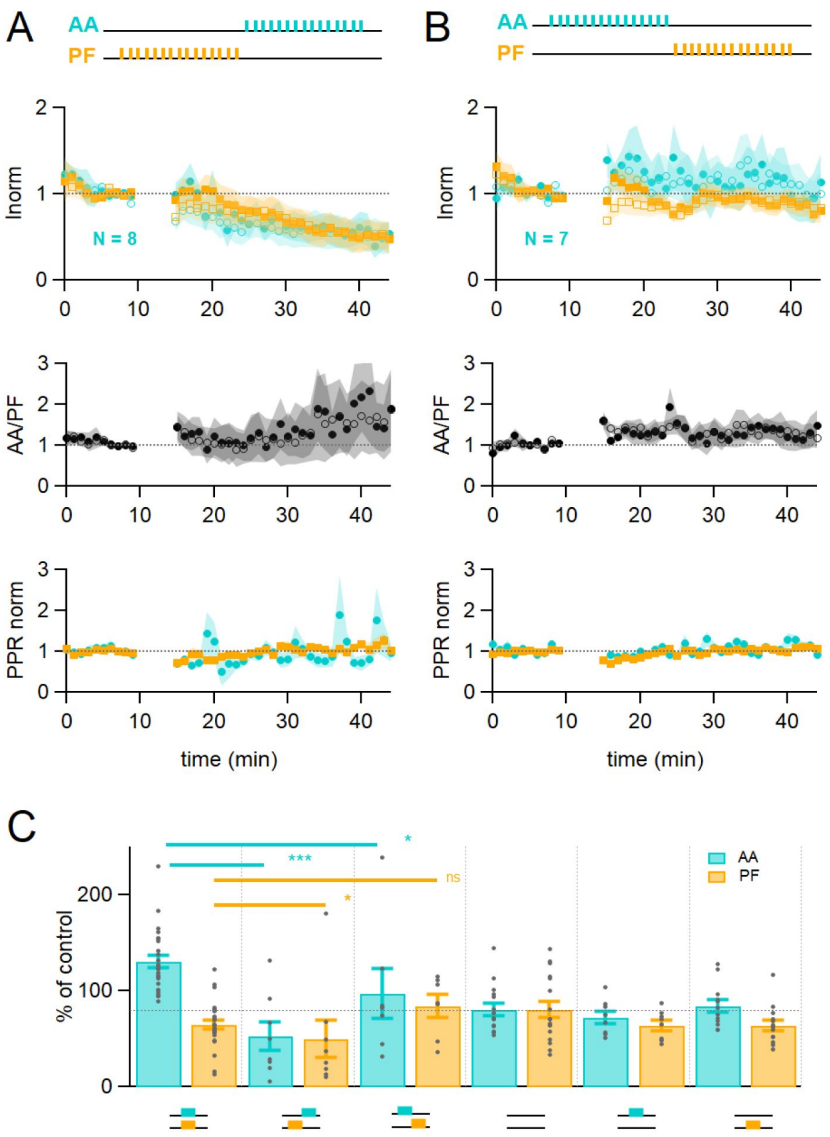

Figure 2

Time dependence of plasticity.

A. On average, when stimulating AAs 150 ms after PFs, the AA- and PF-EPSCs decreased by a similar extent (AA was 53 % ± 15 %, PF 50 % ± 20 % of control, n = 8). The relative normalised amplitude of the AA pathway increased but not significantly (AA/PF was 224 % ± 75 % of control, n = 7). Colour coding for AA and PF input pathways. Closed symbols for the first and open symbols for the second EPSCs. **B**. When stimulating AAs 150 ms before PFs, the AA-EPSC facilitated, but declined back to baseline (AA was 97% ± 26% of control, n = 7), and the PF-EPSC was maintained close to baseline (PF 84 % ± 12 % of control, n= 7). The relative normalised amplitude of the AA pathway and the PPR were not affected significantly (AA/PF was 126 % ± 31% of control, and PPR_{AA} = 114.4 % ± 6.4 %, PPR_{PF} = 107.1 % ± 4.6%, N = 7). **C**. Average amplitude at 25-30 min as a percentage of baseline for various timing of stimulation, control No Stim, AA only and PF only stimulation. Individual data points are overlaid for each type of experiment. The AA-EPSC was 131% ± 7% of baseline (N = 24) 25 to 30 min after induction when AA and PF stimulation was synchronous. It was 53% ± 15% (N = 8) when AA stimulation was delayed by 150 ms, and 97 % ± 26 % (N = 7) when PF stimulation was delayed by 150 ms. The PF-EPSC was 65 % ± 5 % of baseline (N = 25) when stimulation was synchronous, 50% ± 20% (N = 8) when AA stimulation was delayed by 150 ms, and 84 % ± 12 % (N = 7) when PF stimulation was delayed by 150 ms. The horizontal dotted line indicates EPSC amplitude at the end of No Stim experiments. (*** $p \leqslant 0.001$, * $p \leqslant 0.05$, ns: not significant). Values given are mean ± SEM. SEM represented by shading.

are not present postsynaptically at granule cell to Purkinje cell synapses (Llano et al., 1991; Piochon et al., 2007). We investigated the requirement for mGluR1 and NMDAR activation in induction of associative plasticity of the AA and PF pathways.

In **figure 3A** and **B**, mGluR1s were blocked using the competitive mGluR1 antagonist CPCCOEt (50 μM). **Figure 3A** shows a sample experiment in which both the EPSCs and the delayed IPSCs decreased following induction. In these conditions, on average the AA-EPSC increased transiently following induction, but there was a long term decrease within 25-30 minutes (AA was 72% ± 13% of baseline, statistically smaller than control synchronous stimulation, p=0.0004, N=7 and N=24), and the PF-EPSC was also decreased (PF was 54% ± 8 %, N=7, not significantly smaller than control synchronous stimulation, p=0.12, N=7). The transient decrease in PPR was present also in these conditions and for both inputs, indicating no involvement of the mGluR1 in this process.

Figure 3C shows the effect of inhibiting NMDARs with the NMDAR competitive antagonist APV (50 μM) on associative AA and PF plasticity induction. With NMDARs blocked, AA-LTP observed after synchronous stimulation was completely suppressed. The AA- and PF-EPSCs were on average 50% ± 8 % and 40% ± 9% of baseline 25 to 30 minutes after induction (n = 6, significantly smaller than control p = 2e-6, and n = 7, p = 0.027 respectively). When compared to the PF pathway, depression was not significantly different at AA synapses and there was no relative amplitude change (AA/PF = 109% ± 22%, n = 5, p = 0.34) at 30 min. APV did not affect the transient depression of the PPRs. These data show that NMDAR activation is required for the associative AA-LTP described here.

These results show the concomitant involvement of both mGluR1s and NMDARs in the induction of plasticity at GC synapses.

Role of inhibition

PCs receive GABAergic inhibition from molecular layer interneurons directly recruited by GCs. $GABA_A$Rs are also present on GCs, including presynaptically on the GC axon (Stell et al., 2007). These presynaptic $GABA_A$Rs are activated by synaptic release of GABA and affect the axonal Cl^- concentration and synaptic release (Stell et al., 2007; Astorga et al., 2015; Berglund et al., 2016). Several recent studies have shown that plasticity of PF-EPSCs is affected by GABAergic inhibition. Binda et al. (2016) showed that PF-LTP in mice relies on $GABA_A$R activation to hyperpolarize PC dendrites and allow recruitment of T-type Ca^{2+} channels. Rowan et al. (2018) also showed that the recruitment of molecular layer interneuron mediated inhibition can modify CF-mediated Ca^{2+} signals and LTD induction.

The role of $GABA_A$Rs-mediated inhibition was tested during plasticity induction. To this end, a series of experiments was performed with the $GABA_A$R antagonist SR95531 (3 μM) in the bath throughout the recording, and the AA and PF pathways were stimulated simultaneously (**Fig. 4**). The sample experiment in **Figure 4A** shows that the AA-EPSC was slightly increased, while the PF-EPSC was decreased. On average with $GABA_A$Rs blocked, the AA-EPSC was initially facilitated after induction (170% ± 30%, N=9), but that potentiation decreased with time and it was 117% ± 24% of baseline after 25-30 minutes. The outcome of induction on the AA pathway was highly variable, and in 2 out of 9 cells, the AA-EPSC was strongly depressed at 25-30 min. On average, AA-LTP was smaller than in control experiments, but given the variability observed, it was not significantly different from control experiments (p=0.1). The decrease of the PF-EPSC at 25-30 min (56±10%, N=9) was not significantly smaller than control values (p=0.19). The relative plasticity of AA and PF inputs was stable following induction (AA/PF = 330% ±130 % at 25-30 min after induction N=9). The PPR of both pathways was transiently decreased. $GABA_A$R activation therefore seems to be required for efficient induction and maintenance of this type of associative plasticity.

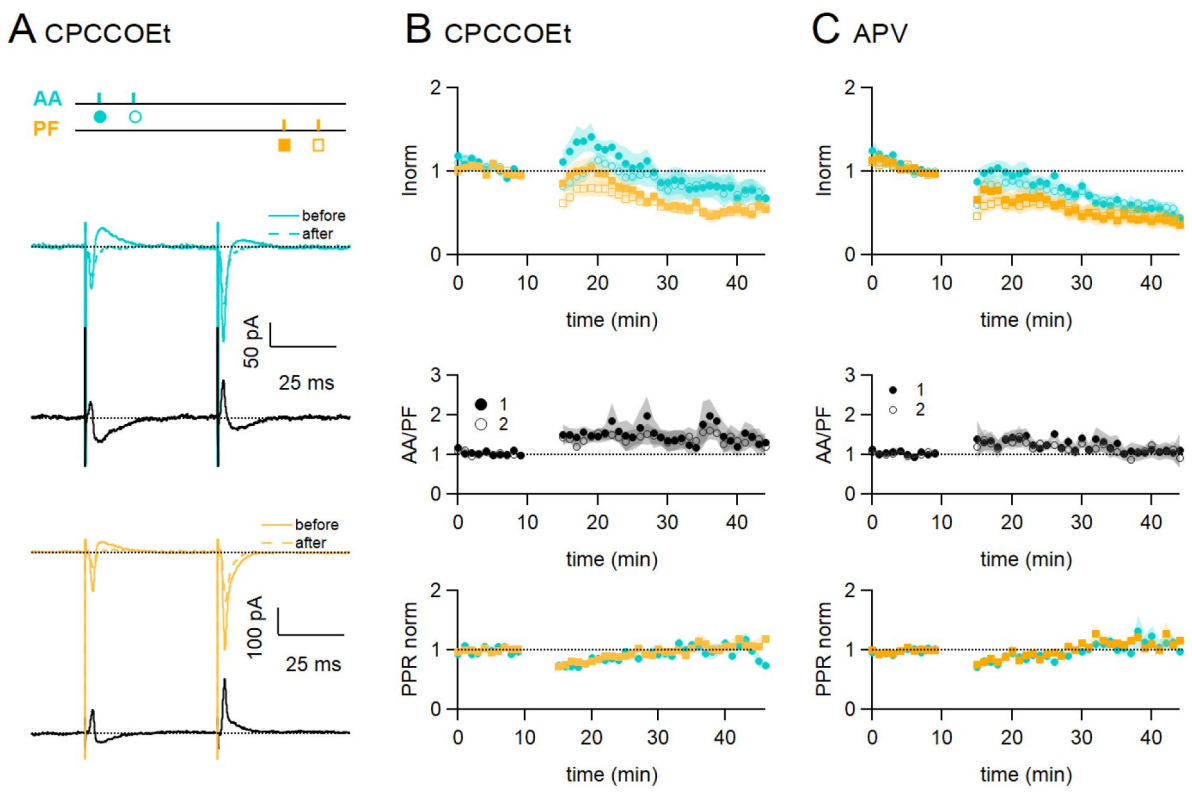

Figure 3

Role of NMDARs and mGluR1s.

A. Bath application of CPCCOEt (50 μM), a selective blocker of mGluR1Rs, strongly inhibits LTP of AA-EPSCs. Sample recordings from one experiment. Traces are the average of the AA (blue) and PF (orange) synaptic responses, before (5-10min, continuous line) and after induction (25-30 min, dotted line). Subtraction traces (25-30 min - 5-10min) in black. A decrease of the AA-EPSC and PF-EPSC is observed. The test stimulation protocol is depicted with colours and symbols as used in the plots in the following sections for the first (closed) and the second EPSCs (open). **B. Top**: Average time course of the normalised AA- and PF-EPSCs (N = 8). mGluR1receptor block impairs AA-LTP. **Middle**: a small sustained increase of the ratio of normalised amplitudes (AA/PF) is observed. **Bottom**: Plot of the normalised PPR of both inputs. **C. Top**: Average time course of the normalised AA- and PF-EPSCs (colours and symbols as in A) in the presence of APV (50 μM) (N = 7). Both AA and PF pathways are depressed, showing that NMDAR activation is necessary for AA-LTP induction. **Middle**: The ratio of normalised amplitudes (AA/PF) is slightly increased, reflecting a slower depression of the AA inputs. **Bottom**: Plot of the normalised PPR of both inputs. Values given are mean ± SEM. SEM represented by shading.

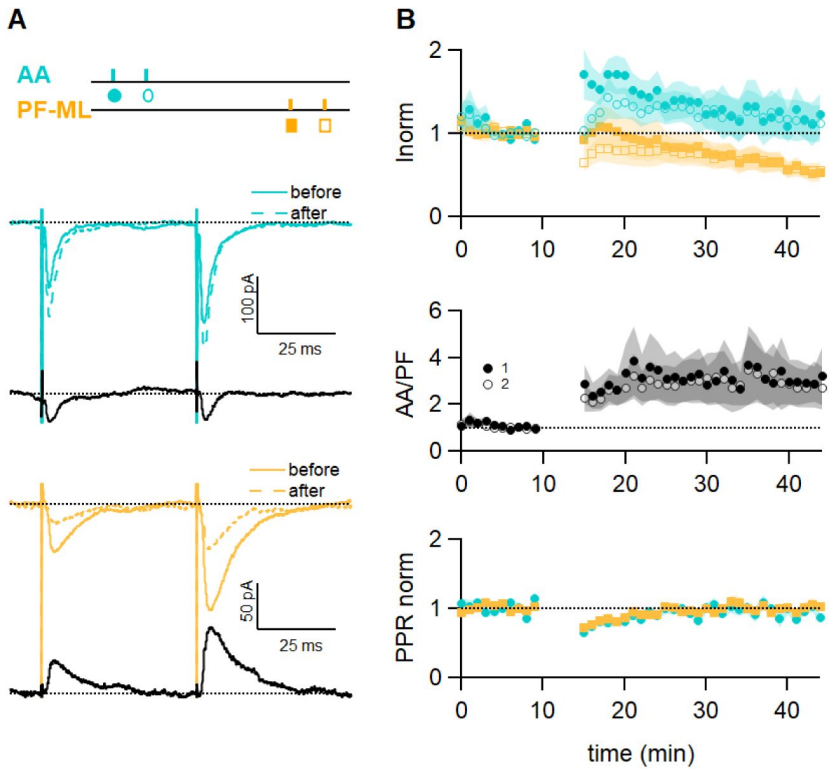

Figure 4

GABAA receptor block affects long term plastic changes.

A. Sample recordings from an experiment in the presence of the $GABA_AR$ antagonist SR (3 μM). Paired EPSCs evoked before and after induction, together with subtraction traces (black), are shown for the AA (blue) and PF (orange) pathways. The AA-EPSC is increased after induction and the PF-EPSC is strongly decreased in this experiment. The test stimulation protocol is depicted with colours and symbols as used in the plots in the following section for the first (closed) and the second EPSCs (open). **B.** Average time course of the normalised AA- and PF-EPSCs (N = 9). The big errors in AA peak amplitude observed after induction are due to the large variability of the outcome of the protocol on this pathway (AA 117%± 24 % ; PF 56%± 10%, n = 9). The ratio of the normalised AA and PF amplitude shows the same variability, while the normalised PPR displays the same relative error and time course as control experiments. Values given are mean ± SEM. SEM represented by shading.

Role of synaptic inputs distribution

We have shown that paired stimulation of AA and PF triggers AA-LTP. AAs can make several synapses per axon, and these are sparsely distributed on the vertical axis of the PC dendritic tree. On the other hand, because PFs are stimulated in the molecular layer, they are stimulated as a dense beam of fibres and therefore a dense patch of synapses. We asked whether induction of AA-LTP is due to the sparse distribution of AA synapses rather than the specific properties of AA inputs.

To test for the role of the sparse distribution of the inputs, a series of experiments was performed substituting local AA stimulation with GC layer stimulation at a distance of 100 to 180 µm from the recorded PC. In this configuration, GC layer stimulation recruits PF synapses sparsely distributed on the PC dendrites and cannot involve AA synapses. The induction protocol was then applied to the sparse PF pathway (PF-sparse), together with the dense pathway stimulated in the molecular layer (PF-dense) (see **Fig. 5A**). **Figure 5B** shows an example of an experiment. Traces show the PF-sparse and -dense EPSCs before and after the induction protocol and subtractions (grey) to highlight changes. 25 to 30 minutes after induction, both the sparse and dense EPSCs are reduced. **Fig. 5C** shows the average time course of 10 experiments. Both the sparse and dense inputs are reduced on average to 88 % ± 13% of baseline (significantly smaller than control AA, p = 0.0024, n= 10 PF-sparse and n= 24 AA control) and 54% ± 10 % of baseline (significantly smaller than control PF, p = 0.017, n= 10 PF-dense and n = 25 PF control) after 25-30 minutes respectively. When AA stimulation was replaced by sparse PF stimulation, the amplitude of the PF-sparse input was not increased as seen for AA inputs, but depressed. There was initially no change of the ratio of normalised amplitudes of the two pathways, although with time, the dense PF input stimulated in the molecular layer was more strongly depressed than the sparse input, and the relative plasticity of PF-sparse increased (PF-sparse/PF-dense = 182 % ± 24 %).

These experiments suggest that associative LTP of the AA input is not due to the sparse distribution of stimulated AA synapses on PC dendrites, but to the stimulation of a population of synapses prone to a specific form of plasticity.

Discussion

We show for the first time that stimulating AA and PF inputs simultaneously triggers LTP of the stimulated AA inputs specifically. AA-LTP is associative as it is not observed with stimulation of either pathway alone and it is timing-dependent. AA-LTP is weakly dependent on GABAergic inhibition, but most interestingly also, it depends on the activation of both mGluR1s and NMDARs. It is linked to the identity of AA synapses rather than their sparse distribution on PC dendrites, as it is not observed for sparse PF inputs. Below we discuss these findings and potential consequences for cerebellar physiology.

Identification of AA synapses

We have shown that the difference in plasticity observed between the AA and PF inputs is not linked to the distribution of synapses on the dendritic tree but to different properties of the synapses. We have argued earlier that our approach for stimulating fibres recruits mainly PF synapses, for molecular layer stimulation, and mainly AA synapses, for local GC layer stimulation. However, we have no morphological identification to verify that all stimulated synapses are strictly AA or PF synapses. Strictly speaking, GC layer stimulation close to the PC soma will recruit synapses from local GCs, formed by the initial portion of the axons, including some formed by the PF close to the bifurcation point, whereas molecular layer stimulation will recruit mostly synapses from distal GCs and formed by the distal portion of the axons. The observed associative plasticity

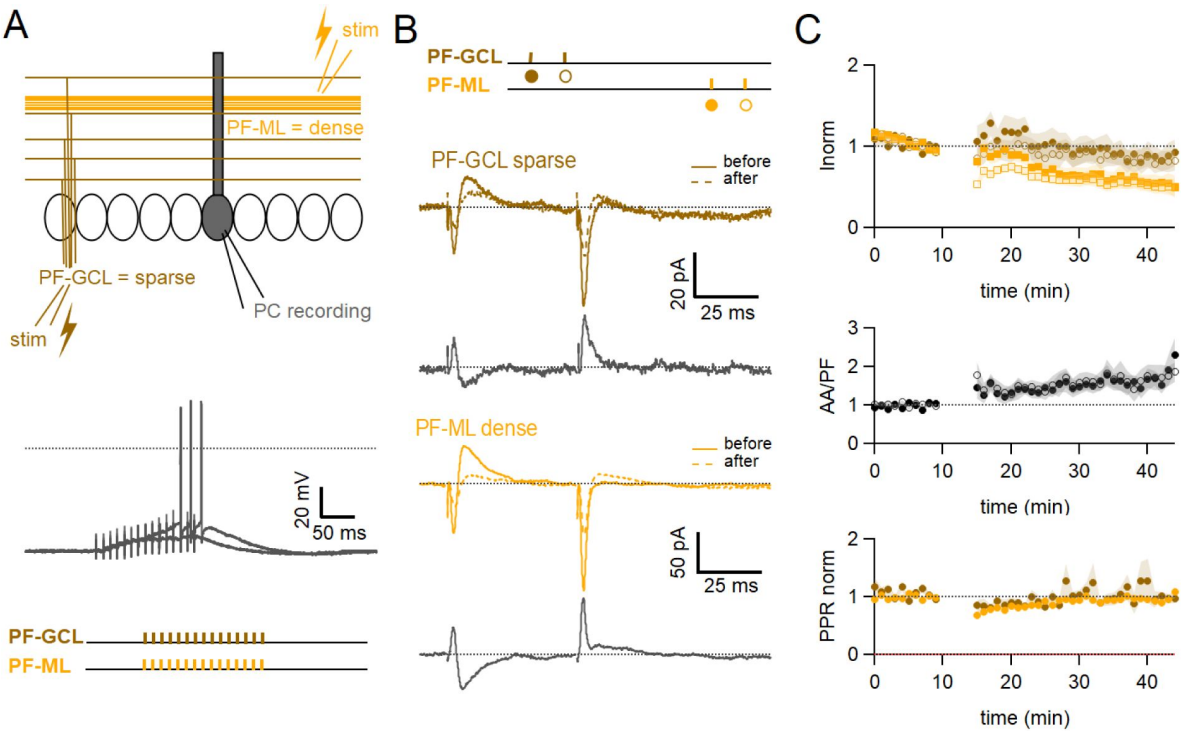

Figure 5

Role of the sparse input distribution.

A. To test the role of the sparse input distribution, a stimulation electrode was positioned in the GC layer, stimulating only PF synapses sparsely distributed on the PC dendrites. The induction protocol was applied to the sparse PF pathway (PF-sparse), together with the dense PF pathway stimulated in the molecular layer (PF-dense). **B.** Example experiment. Traces show the PF-sparse and -dense EPSCs before and after induction, and subtractions (grey) to highlight changes. The test stimulation protocol is depicted with colours and symbols as used in the plots in the following section for the first (closed) and the second EPSCs (open). 25 to 30 minutes after induction, both the sparse and dense EPSCs are reduced. **Bottom left**, IClamp responses to the first two trains of stimulation. **C.** Average time course of the normalised EPSC amplitudes (N = 10). Both sparse and dense inputs are reduced on average to 88 % ± 13% (significantly smaller than control AA, p = 0.0024, n= 10 PF-sparse and n= 24 AA control) and 54% ± 10 % of baseline (significantly smaller than control PF, p = 0.017, n= 10 PF-dense and n = 25 PF control) after 25-30 min respectively. With time, the dense PF input was more strongly depressed, and the ratio of normalised amplitudes (PF-sparse/PF-dense) increased to 182 % ± 24 % of control. Values given are mean ± SEM. SEM represented by shading.

could thus alternatively be due to a gradient of properties of synapses from proximal to distal sites along the GCs axon. If there is a gradient however, it is limited to short distances compared to the total fibre length, as this effect was not observed when stimulating PFs in the GC layer 100-180 µm from the recorded cell (4 to 5% of the total fibre length, **Fig. 5**). If the plasticity described here applies to a gradient along the GC axon rather than to AAs and PFs, this would not impact the mechanisms identified nor the consequences for cerebellar physiology.

AA plasticity

We have observed AA-LTP with synchronous stimulation and AA-LTD when AAs were stimulated 150 ms after PFs (**Fig. 2**). To our knowledge, only Sims and Hartell (2005, 2006) examined plasticity at AA synapses and reported the absence of both LTP and LTD associated with CF conjunctive stimulation.

For both AA and PF pathways, the PPR transiently decreased following the induction protocol. Changes of the PPR have been linked to a change of the presynaptic release probability (Zucker and Regehr, 2002). This suggests a transient presynaptic effect following induction, which likely explains the progressive changes of AA and PF responses. Presynaptic $GABA_B$ and CB1 receptors have been shown to modulate the presynaptic release probability at granule cell to Purkinje cell synapses, but they decrease release and increase the PPR (Dittman and Regehr, 1997; Safo and Regehr, 2005). Also, endocannabinoid release is triggered by mGluR1 activation, but mGluR1 block did not affect the transient decrease of the PPR. Therefore activation of these receptors cannot account for the transient presynaptic effect we observed. However, there was no significant long term change of the PPR, suggesting that AA-LTP is due to postsynaptic changes.

Activation of both mGluR1s and NMDARs was required for AA-LTP induction (see **Fig. 3**). This is interesting in view of the past involvement of these receptors, mostly independently, in postsynaptic forms of cerebellar PF LTD and LTP, both linked to PF stimulation (Daniel et al., 1992; Konnerth et al., 1992; Hémart et al., 1995; Lev-Ram et al., 1997; Casado et al., 2002; Safo and Regehr, 2005; Bidoret et al., 2009; Bouvier et al., 2016). The difference with previous reports lies with the simultaneous stimulation of AA with a PF beam. The conjunctive requirement for NMDAR and mGluR1 activation could be explained based on the dependence of plasticity on the concentrations of both NO and postsynaptic calcium (Coesman et al., 2004; Safo and Regehr, 2005; Bouvier et al., 2016; Piochon et al., 2016). NO production has been linked to the activation of NMDARs in granule cell presynaptic boutons (Casado et al., 2002; Bidoret et al., 2009; Bidoret et al., 2015; Bouvier et al., 2016), or occasionally in molecular layer interneurones (Kono et al., 2019). NO is a diffusible messenger and it activates the Guanylate Cyclase in the postsynaptic Purkinje cell. On the other hand, mGluR1s in Purkinje cells are strongly linked to Ca^{2+} signalling. They activate several downstream pathways, including IP_3-mediated Ca^{2+} release from stores (Finch & Augustine, 1998; Takechi et al., 1998), a slow EPSC mediating calcium entry (Canepari et al., 2004; Canepari and Ogden, 2006) and regulate voltage activated Ca^{2+} channels (Hildebrand et al., 2009; Otsu et al., 2014; Ait Ouares et al., 2020)), all leading to an increase of the postsynaptic calcium concentration. NMDARs and mGluR1s could cooperate to control postsynaptic plasticity (see Diagram 1A).

Presynaptic NMDAR and postsynaptic mGluR1 activation could take place at AA and PF synapses independently. However, the need for coincident activation of the two synaptic inputs suggests either spatial overlap or a requirement for crosstalk between the two synaptic territories. Our experiments used horizontal slices, where PC dendrites dip into the slice, so we have no indication whether the two synaptic territories overlap. Given the size of the synaptic currents (Suppl. Fig. 2) however, they represent a small number of synapses compared to the total number formed by granule cells on a PC. The median PF-EPSC (288 pA, n = 25) corresponds to approximately 34 active synapses (unitary amplitude for distal GC to PC connection is 8.4pA (Isope and Barbour, 2002)). Taking into account that 85% of the synapses formed by PFs onto GCs are silent, our stimulation likely recruits about 230 synapses, active and silent, put together. For a similar unitary synaptic

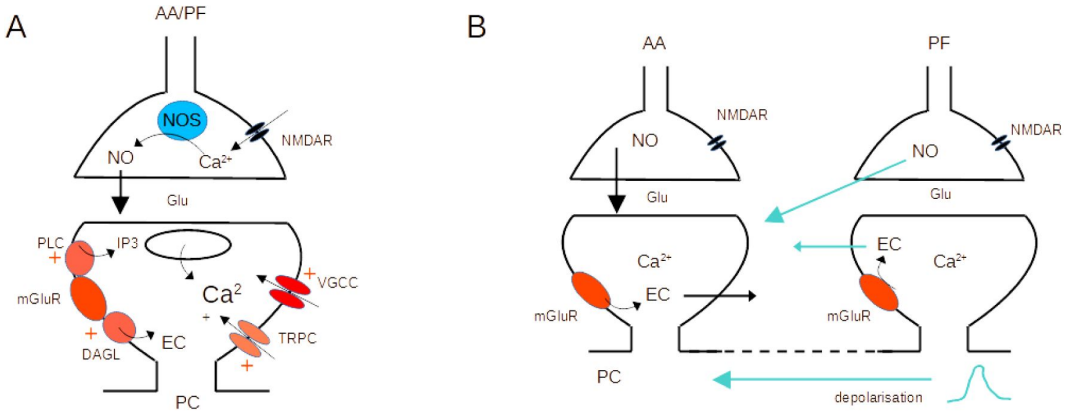

Diagram 1

Molecular pathways and potential crosstalk mechanisms involved in AA-LTP.

A. Activation of presynaptic NMDARs triggers Ca2+ entry, activation of NOS and production of NO. NO diffuses to the postsynaptic compartment where it triggers Guanylate Cyclase activation and regulation of AMPAR number. Activation of postsynaptic mGluR1s in the PC activates PLC, DAGL, TRPC and a modulation of VGCC, triggering an increase of the Ca2+ concentration and EC production. NO and Ca^{2+} concentration control plasticity (Bouvier et al., 2016). **B.** The dendritic depolarisation triggered by activation of the dense patch of PF synapses might prime Ca^{2+} release from stores linked to mGluR1 activation. Alternatively, NO or EC produced at PF synapses might diffuse to AA synapses. Potential sources of crosstalk are highlighted in blue.

AA ascending axon, DAGL Diacylglycerol lipase, EC Endocannabinoids, Glu glutamate, NO Nitric Oxide, NOS Nitric Oxide Synthase, PC Purkinje cell, PF parallel fibre, PLC phospholipase C, TRPC Transient receptor potential canonical channel, VGCC voltage gated calcium channels.

size, the median AA-EPSC (90 pA) would correspond to 11 active synapses and a total of 22 synapses (50% of local GC to PC connections are silent (Isope and Barbour, 2002)). These numbers represent less than 0.2% of the 175 000 excitatory synapses present on the dendritic tree of a PC (Napper and Harvey, 1988). Given that we placed the PF stimulating electrode at variable depths and distances from the recorded Purkinje cell, there is statistically little chance of reproducible overlap between the territories of PF and AA recruited. Moreover, AA synapses will be spread in the vertical axis of the dendrites whereas PF synapses will form a dense patch on the PC dendrites. Spatial overlap is therefore unlikely to happen in a significant proportion of experiments, suggesting that for interaction to occur a signal needs to propagate from PF to AA synapses to explain associative AA-LTP.

Crosstalk might be required because a receptor is absent from AA synapses or a pathway fails to activate. The specific localisation of receptors at AA vs PF synapses is unknown. If mGluR1 is present at AA synapses, stimulation could activate the mGluR1 slow EPSC or mGluR1 mediated presynaptic endocannabinoid inhibition. However, this is not observed at sparse PF inputs unless glutamate transporters are blocked (Marcaggi and Attwell, 2005), which is thought to reflect insufficient glutamate buildup, and makes it difficult to localise the receptors. mGluR1 mediated Ca^{2+} release from stores shows a higher sensitivity to glutamate (Canepari and Ogden, 2006) and might take place with sparse inputs, but Ca^{2+} signals have not been investigated in this configuration, and we do not know if mGluR1s are present at AA synapses. Similarly, we do not know whether presynaptic NMDARs are present.

A crosstalk mechanism would require propagation of a signal between synaptic territories. mGluR1-mediated Ca^{2+} signals in Purkinje cells are not expected to propagate across the PC dendritic tree, because both Ca^{2+} and IP_3 are quickly buffered. On the other hand, mGluR1-mediated Ca^{2+} release from stores is known to require priming by depolarisation (Canepari and Ogden, 2006). It is possible that mGluR1s are present at AA synapses, but Ca^{2+} release fails to activate because the local depolarisation is insufficient. The PF beam stimulated forms a dense patch of synapses which will be very efficient at depolarising the membrane potential locally, and this depolarisation might spread to AA synapses if it reaches threshold for active conductances. Fluctuations of the dendritic membrane potential triggered by the PF-EPSC might enable mGluR1-mediated Ca^{2+} signals at AA synapses. The isolation of AA synapses in fine dendritic branches (Lu et al., 2009) might make them more prone to depolarisation. mGluR1 activation also triggers the production of endocannabinoids (EC; Maejima et al., 2001; Brown et al., 2003), and presynaptic CB1Rs have been involved in PF-LTD (P. K. Safo & Regehr, 2005; Carey et al., 2011). Similarly, NO is released by the activation of presynaptic NMDARs. EC and NO are both diffusible messengers and potential substrates for crosstalk between AA and PF synapses. Activation of PF synapses might be required for NO or EC production and diffusion to AA synapses (See Diagram 1 for potential crosstalk mechanisms). Further experiments will be required to test whether EC or NO are sufficient to induce AA-LTP when stimulating AA inputs on their own.

PF synapses

In the experimental conditions used here, the induction protocol had no significant effect on the amplitude of the PF-EPSC although we observed a tendency to decrease. This was unexpected because the induction protocol we used, when applied to PF only and with inhibition preserved, was previously shown to induce PF-LTP (Binda et al., 2016; Jörntell & Ekerot, 2002), although not always (Gonzalez-Calvo et al., 2021). But Binda et al. (2016) also showed that PF-LTP was not sustained when inhibition was blocked during induction, contradicting other studies performed with inhibition blocked (Bouvier et al., 2016; Piochon et al., 2016; Schonewille et al., 2021) with Picrotoxin or Bicuculline (a blocker of SK channels, Khawaled et al., 1999). Moreover, PF-LTP either relied on mGluR1 activation (Binda et al.,2016), or NMDAR activation (Bidoret et al., 2009; Bouvier et al., 2016; Schonewille et al., 2021). Therefore, we do not have an explanation for the lack of PF-LTP, but the literature shows multiple contradictions, likely indicating that the processes involved are sensitive to the experimental conditions. Noticeable

experimental differences with the study of Binda (2016) are the use of mice rather than rats, differences in the orientation of cut of the slices, which might have resulted in the study of different cerebellar lobules, but importantly also, we used a low internal Cl^- concentration, reproducing the concentration estimated in PCs (Chavas & Marty, 2003), and the recording solution was supplemented with 10 µM of the Ca^{2+} buffer EGTA.

Role of inhibition

Experiments were performed with inhibition preserved and $GABA_A$Rs activation was shown to secure efficient induction of AA-LTP (see **Fig. 4**). Block of $GABA_A$Rs did not suppress the initial increase in amplitude, but under these conditions plasticity was not sustained, highly variable and not significant when compared to control experiments. Inhibition indeed seems to interfere with plasticity induction (Binda et al., 2016; Rowan et al., 2018). At this stage, we have no detail on the mechanism of influence of GABAergic inhibition in AA-LTP induction. Binda et al. (2016) showed that hyperpolarisation by IPSCs relieves inactivation of T-type Ca^{2+} channels, themselves regulated by mGluR1, boosting Ca^{2+} signals and triggering PF-LTP. That mechanism would seem compatible with our results at AA synapses although we do not know whether it requires NMDARs activation. On the other hand, the work by Rowan (2018) indicated that inhibition decreased Ca^{2+} entry, and as a result converted LTD into LTP. In this study, inhibition was recruited using optogenetics rather than synaptic excitation, and it is possible that the pattern of inhibition generated was less physiological, both with respect to the number of molecular layer interneurons stimulated and timing. This might explain the different results.

Cerebellar physiology

We argued in the introduction that, as a consequence of morphology, AAs can only form synapses with a few PCs, while PFs course through and synapse with the dendrites of hundreds of PCs. AA synapses are suited to encode precise and selective information from the receptive field, while PF synapses could efficiently represent context. This work is consistent with the idea that they are functionally different and might fulfil distinct roles with respect to the computation performed by the cerebellar cortex. The associative form of plasticity we describe, together with the time dependence, is expected to reinforce AA signals presented conjointly with PF, or within a pertinent time window, while attenuating signals presented in isolation. This would lead to strengthening of the inputs linked to activity in other receptive fields.

This work shows that associative plasticity in PCs can be triggered by granule cell inputs independently of the climbing fibre, requiring only moderate inputs, in contrast with the powerful CF, which triggers widespread depolarisation and Ca^{2+} increase. The climbing fibre is classically associated with error signals and learning (Albus, 1971; Ito and Kano, 1982; Marr, 1969; Medina and Lisberger, 2008; Yang and Lisberger, 2014). However, both climbing fibre (Kostadinov et al., 2019) and granule cells (Wagner et al., 2017) have been shown to encode reward signals, which might be important in driving plasticity.

Acknowledgements

We would like to dedicate this work to the memory of David Ogden, who was influential in placing the cerebellum at the centre of this work. We thank Brandon Stell and Alain Marty for discussions on the manuscript. We thank the Animal Housing and Breeding facility and the Prototyping facility of BioMedTech facilities (INSERM US36, CNRS UAR2009, Université Paris Cité) for providing the animals used in this study and assistance with technical developments. The work was funded by ANR grants ANR-19-CE37-011-01 SpinoCereLoco and ANR-18-CE16-0010-01 RewardInhib.

Methods

Ethical approval

Sprague Dawley rats were provided by Janvier (St Berthevin, France) or bred and subsequently housed at the Animal Housing and Breeding facility of BioMedTech facilities (INSERM US36, CNRS UAR2009, Université Paris Cité) in agreement with the European Directive 2010/63/UE regarding the protection of animals used for experimental and other scientific purposes. Experimental procedures were approved by the French Ministry of Research and the ethical committee for animal experimentation of Paris Cité.

Slice preparation

Experiments were performed on horizontal slices 300 µm thick cut from the cerebellum of 19-25 day-old Sprague-Dawley male or female rats. Briefly, rats were killed by decapitation under general anaesthesia following inhalation of the volatile anaesthetic isoflurane at a concentration of 3-4% in accordance with the Directive 2010/63/UE, and the cerebellum was quickly removed. After removal of the brainstem, the tissue was glued to the stage of a vibratome (Leica VT1200S, Germany). Slices were cut at a temperature of 34° C and subsequently kept in a vessel bubbled with 95% O_2 / 5% CO_2 at this temperature. Slice preparation and recordings were made in a bicarbonate buffered solution containing in mM: 115 NaCl, 2.5 KCl, 1.3 NaH_2PO_4, 26 $NaHCO_3$, 2mM $CaCl_2$, 1mM $MgSO_4$, 0.1mM Ascorbic Acid, and 25 glucose.

Patch-clamp recording of synaptic currents

Whole-cell patch-clamp recordings were made from PCs, identified by their size and location at the edge of the molecular and GC layers, with an EPC10 amplifier (HEKA, Germany) and PatchMaster acquisition software. Bath temperature was kept at 30-32° C The internal solution contained in mM: 135 KGluconate, 10 K_2 Creatine Phosphate, 10 HEPES, 0.01 EGTA, 2.5 $MgCl_2$, 2 $ATPNa_2$ and 0.4 GTPNa, pH adjusted to 7.3 with KOH and osmolarity to 295 mOsm/kg. When filled with the internal solution, recording pipettes had a resistance between 3 and 4 MΩ. Membrane currents were recorded at a pipette potential of -60 mV (not corrected for junction potential of approximately -12 mV pipette-bath). Series resistance was 80-90 % compensated. During experiments, the preparation was visualised on an upright microscope (Olympus BFX51; 60x 0.9 NA water dipping objective) and the bath was continuously perfused at a rate of 5 ml/min (5 bath volumes per min) with solution equilibrated with 95% O_2 / 5% CO_2 to maintain pH and solution recirculated.

Plasticity of GC to PC synapses was studied in horizontal cerebellar slices as these slices better preserve PFs running in the plane of cut. At this age, GC synapses are well established (Ichikawa et al., 2016). AAs and PFs were stimulated with patch pipettes slightly larger than those used for recordings filled with a Hepes-buffered external solution and positioned either in the molecular (lower two thirds) or the GC layer, as discussed in the result section. The baseline amplitude of both AA and PF pathways were sampled with a pair of suprathreshold pulses at 50 ms interval, delivered every 10 s (**Fig 1A** top panel, stimulation was biphasic, 100-180 µs duration, 5 to 15V). The AA and PF test stimuli were separated by 0.5 s. Stimulation strength was adjusted between 5 and 15V to stimulate AA- and PF-EPSCs reliably. PF stimulation was usually very efficient as fibres are densely packed in the molecular layer and PF-EPSC amplitude typically increased smoothly with stimulation intensity. Although we originally worked with large amplitude PF-EPSCs (up to about 1nA), we aimed at amplitudes of a few hundred pA, closer to the amplitude of stimulated AA-EPSCs, by adjusting stimulation intensity. Granule cell somas and axons are more sparse in the granule cell layer and stimulation intensity was adjusted to activate EPSCs a few hundred pA when possible, but increasing stimulation intensity did not necessarily recruit larger EPSCs. Care was taken to avoid stimulating the local Purkinje cell axon and climbing fibre. Once a stable input was

obtained, stimulation intensity was raised by one Volt to increase reliability. In most of the experiments AAs were tested first to avoid possible interference from mGluR1s activation and the release of endocannabinoid by PFs stimulation. No antagonist of the inhibitory inputs was applied. Evoked responses consisted of excitatory postsynaptic currents (EPSCs) that were often quickly followed by inhibitory postsynaptic currents (IPSCs) (mixed EPSC/IPSC, see supplementary material and supplementary fig.3). The low Cl^- concentration in the intracellular solution ensured the reversal potential for Cl^- was close to the value determined for PCs (-85 mV, (Chavas & Marty, 2003)), and IPSCs were outward at the recording potential of -60 mV. After recording a baseline period of at least 10 minutes, we applied a stimulation protocol aimed at inducing plasticity. The recording configuration was switched to Current clamp and the potential set and maintained near -65 mV. The protocol applied (see **Fig. 1A** bottom panel) consisted in the synchronous stimulation of both inputs by a train of 15 pulses at 100 Hz repeated every 3 s a total of 100 times. Following the induction protocol, the recording configuration was returned to Voltage clamp and test of alternate AA- and PF-EPSC amplitude resumed. In the result section the number of cells sometimes differ for the two pathways for a given set of experiments, because one of the inputs was sometimes lost during the 30 minutes following induction. Because the protocol was properly applied, the data for the remaining input were included in the results.

Analysis of evoked EPSCs

For the analysis of synaptic currents, raw current traces were exported to Igor Pro (Wavemetrics) and peak excitatory current amplitudes were measured as the minimum of the synaptic response (mixed EPSC/IPSC) over a time window overlapping the peak and spanning a few sampling points of the average EPSC. Since the plasticity protocol might affect EPSCs and IPSCs differently, and might therefore affect our estimate of the peak EPSC and its long term changes, we conducted a set of experiments to measure the IPSCs and EPSCs separately and confirmed that measuring the minimum of the mixed EPSC/IPSC gives a good estimate of EPSC amplitude and its long term changes (see supplementary materials and supplementary figure 3).

Chemicals

2-(3-Carboxypropyl)-3-amino-6-(4methoxyphenyl)pyridazinium bromide (SR 95531), D-(-)-2-Amino-5-phosphonopentanoic acid (D-AP5) and 7-(Hydroxyimino)cyclopropa[b]chromen-1a-carboxylate ethyl ester (CPCCOEt) were purchased from Tocris Bioscience or from HelloBio (UK). CPCCOEt was dissolved in DMSO at a concentration of 100mM. All other stocks were prepared in water. Drugs were diluted in saline just before use. All other chemicals were purchased from Sigma.

Statistical significance

was tested with non-parametric methods for most of the data sets. These do not require assumptions about the nature of the distribution of the variables (as parametric tests do); we used either the Wilcoxon signed rank test (non-parametric, for paired samples) or the Wilcoxon Mann Whitney test (non-parametric, for unpaired samples). The T-test was used for control data only, where N was big enough to show a normal distribution of the variables (see Supplementary figure 2). Tests were conducted using Igor Pro (Wavemetrics). All values given are mean ± SEM.

Supplementary material

Control No Stim experiments

A series of control experiments was conducted to quantify the rundown of the EPSC amplitude. Following baseline sampling, recording was switched to Iclamp for 5 min, as done during the induction protocol, but no stimulation was delivered during that period.

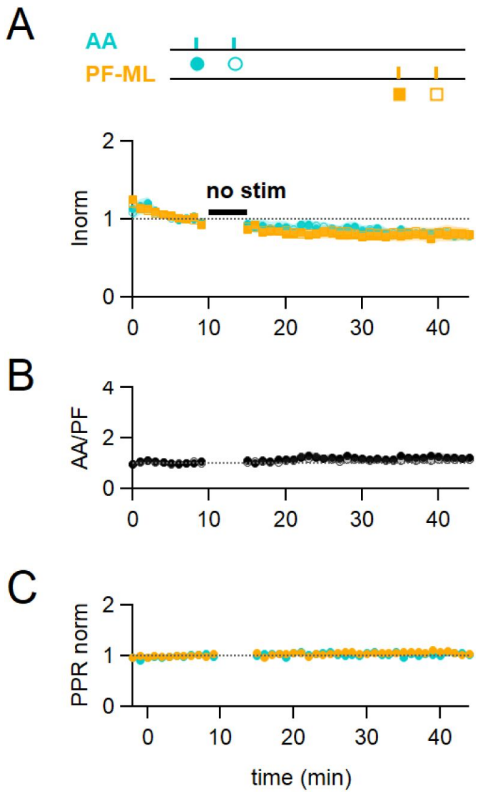

Supplementary Figure 1

Control No Stim experiments.

A, plot of the average AA- and PF-EPSC amplitude normalised to baseline (n = 17, colours and symbols shown on the experimental protocol). No stimulation was applied during the 5 min IClamp period. Rundown of the AA- and PF-EPSCs peak amplitude was observed throughout the experiments. On average, the amplitude of the AA-EPSC and PF-EPSC decreased to 80 ± 6% (n= 16, significantly smaller than baseline p = 0.0004) and 81 ± 8% (N = 17, not significantly smaller than baseline p = 0.062) of baseline 25-30 min after induction respectively, indicating a rundown of the amplitude for both pathways during experimental time, independent of the induction protocol. **B**, average ratio of the normalised amplitudes of AA- and PF-EPSCs showing relative stability of the inputs following the No Stim protocol. **C**, average normalised paired pulse ratio (AA2/AA1 and PF2/PF1) is unchanged.

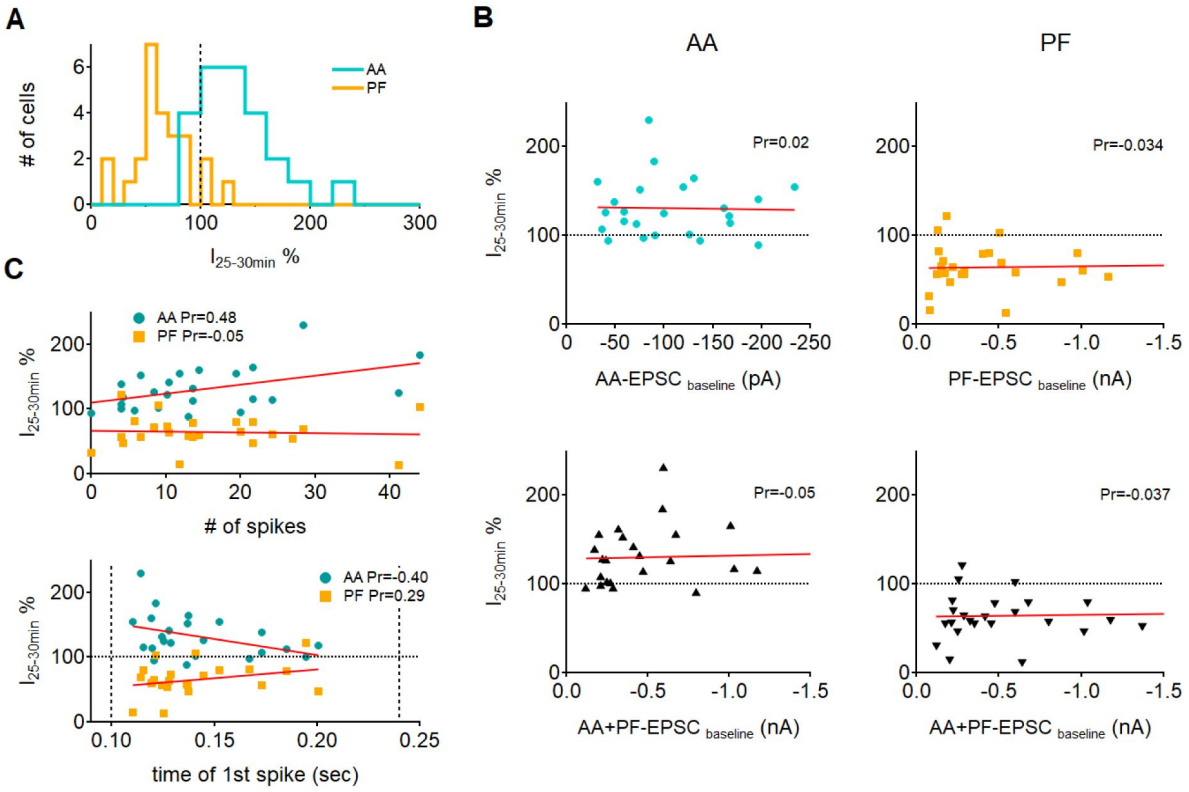

Supplementary figure 2

Effect of EPSC amplitude and spiking of the Purkinje cell on plasticity.

A. Histogram showing the distribution of long term changes of AA- and PF-EPSCs for all control cells. Data is normally distributed. **B**. Top: plots of long term changes of AA- and PF-EPSCs amplitudes for control cells as a function of the baseline EPSC amplitude (n = 24 for AA and n=25 for PF). The red line represents the linear fit of the data. No correlation was observed between plastic changes and the initial amplitude of the response, as indicated by the Pearson's coefficients of linear regression (Pr). Bottom: long term changes plotted as a function of the sum of baseline AA and PF amplitudes to check for a cooperative effect of the inputs. Again, no correlation was found between the long term plasticity outcome and the total amplitude of synaptic currents, as indicated by the linear fits and regression coefficients. **C**. Plots of long term changes in AA and PF amplitudes as a function of the number of spikes evoked by synchronous stimulation during induction (top) and the time at which the first spike was fired (bottom, dotted vertical bars indicate the beginning and end of the stimulus train). For each cell the number of spikes and the time of the first spike are averaged over the first 5 trains of stimulation. The decrease of PF responses was independent of the number of spikes evoked or the time at which the first spike was fired (Pr:Pearson's coefficient of linear regression). For AA responses instead, there was a moderate positive correlation between the level of LTP and the number of spikes, and a moderate negative correlation between the level of LTP and the time at which the first spike was fired, indicating a weak dependence of AA plasticity on spiking during induction.

Analysis of the excitatory and inhibitory components of the mixed response shows no bias due to overlapping inhibition

Our experiments were performed with inhibition intact and with a Cl^- reversal potential close to the value estimated in PCs (-85 mV, (Chavas & Marty, 2003)). Because GCs also synapse on molecular layer interneurons, most of the time AA and PF stimulation recruits monosynaptic excitation and disynaptic inhibition to PCs, generating a mixed synaptic response with excitatory and inhibitory currents of opposite signs, where inhibition comes with a short delay. As a result, the time course of the recorded mixed PSC can be complex. Also, the plasticity protocol might affect EPSCs and IPSCs differently, and the estimate of the peak EPSC and its long term changes might be affected by the overlapping inhibitory currents. To control for possible errors in the estimate of the excitatory peak amplitude, in a set of experiments we made short applications of the $GABA_A$R antagonist SR95531 (SR) before and after induction, to isolate the excitatory from the inhibitory component of the synaptic response. We assumed that the mixed PSCs is the arithmetic sum of two synaptic functions: an EPSC and a delayed IPSC. For the EPSC we used a function of the form:

f(x)=0 for x<xd1

f(x) =A (1-exp(x-xd1)/tr1)^3*exp(x-xd1)/td1 for x>xd1

where x represents time, and A, xd1, td1 and tr1 are the fitting parameters. A is the amplitude, xd1 the delay after stimulus onset, tr1 the rise time constant of the third power exponential rise and td1 the decay time constant of the EPSC. We used a third power exponential rise as it best fitted the data compared to a single or quadratic exponential rise.

For the IPSC we used a function of the form:

f(x)=0 for x<xd2

f(x)=B (1-exp(x-xd2)/tr2)^2*exp(x-xd2)/td2 for x>xd2

where x is time, and B, xd2, td2 and tr2 are the fitting parameters. B is the amplitude, xd2 the delay after stimulus onset, tr2 the rise time constant of the second power exponential rise and td2 the decay time constant of the IPSC. For the IPSC a quadratic exponential rise gave a good fit.

The pharmacologically-isolated EPSCs (measured between 2 to 3 min after SR perfusion) were used to characterise the kinetic parameters of the excitatory responses, and were well described by the fitting function. The fitting EPSC function was then subtracted from the recorded mixed PSC to extract the IPSC component of the response. Since we observed an effect of SR application on the amplitude of EPSCs (presynaptic $GABA_A$Rs are known to modulate release probability (Stell et al., 2007)), the EPSC fitting function was first rescaled to match the rise of the mixed response before subtraction. The resulting inhibitory component of the response was well fitted by the IPSC function and allowed us to estimate its kinetic parameters. Supplementary Figure 3A shows the average time course of the mixed response normalised to the peak EPSC for both AA and PF, and the extracted excitatory and inhibitory components, during baseline for all cells (n=7). The average delays and decay time parameters estimated were: tau-decay: 5±1 msec for excitatory (N=7), 6.5±1.6 msec for inhibitory (N=6) responses for AA stimulation and 4.4±0.6 msec for excitatory (N=7) and 5±1 msec for inhibitory (N=4) responses for PF stimulation; average delay between inhibitory and excitatory current onset: 1.51±0.15 msec for AA stimulation (n=6), and 1.7±0.3 msec for PF stimulation (n=4).

To measure the excitatory and inhibitory components of the evoked mixed EPSC/IPSC before and after the induction protocol, we first recorded the AA- and PF-mixed PSCs for a short control period and then applied the $GABA_A$ receptor antagonist SR95531 (3μM) for 3-4 mins. SR was then washed off the slice for 15 to 20 min, the induction protocol was applied, and the synaptic response was monitored for a further 30 min. SR was applied again to monitor the isolated EPSCs at the end of the experiment. For each experiment, the EPSC fitting functions obtained during the first application of SR were used to calculate the amplitude of the two synaptic components during the period preceding induction (10 min), and those obtained from the second SR application at the end of the recordings, to calculate the amplitudes after induction (30 min). Supplementary figure 3B shows an example of analysis of excitatory and inhibitory components before and after the induction protocol, with mixed PSCs and corresponding excitatory and inhibitory fitting functions, which shows an increase of the AA-EPSC and a decrease of the PF-EPSC, together with an increase of the IPSC in both pathways. In these experiments, the inhibitory disynaptic component evoked by both AA and PF stimulations had a tendency to increase after the pairing protocol, indicating that excitation and inhibition do not necessarily change in the same direction. However, due to the small sample and the absence of an inhibitory component in some of the experiments, long term changes in the inhibitory synaptic components were not significantly different from baseline (average change in peak IPSC: 130± 50 % for the AA pathway, p=0.4 of being bigger than baseline N=5; and 150± 50 % for the PF pathway, p=0.2 of being bigger than baseline, N=4). When measured at the end of the plasticity experiments, the decay time of the excitatory responses estimated were: tau-decay: 7±2 msec (N=7, not significantly different from baseline, p = 0.14) for AA stimulation and 6.0±0.7 msec (N=7, significantly different from baseline, p = 0.026) for PF stimulation.

On average, the plasticity of the AA- and PF-EPSC (measured by the usual method of amplitude of the minimum of the PSC response) in these experiments was not significantly different from that in control experiments (AA pathway: 160 ± 30 %, as compared to 131±7 % in control, p=0.4,N=7 et N=24 and PF pathway 65 ± 9 %, as compared to 65 ± 5 % in control, p=1, N=7 et N=25 for SR and control respectively; ratio of normalised AA/PF responses: 3±1, p=0.76, N=7 et N=24), showing that the short applications of $GABA_A$R antagonist did not influence the plasticity outcome (Supplementary Figure 3C). We thus analysed the change in amplitude of the stimulated pathways using the two separated EPSC/IPSC components obtained by the fitting method before and after the induction protocol to check for differences with respect to the standard method used in all other experiments. Supplementary figure 3D compares, for each cell, the AA- and PF-EPSCs relative amplitudes obtained by direct measure of the mixed PSC minimum with those obtained with the fitting method. The two methods of measurements are equivalent. The delayed onset of the inhibitory component limits its impact on the EPSC amplitude.

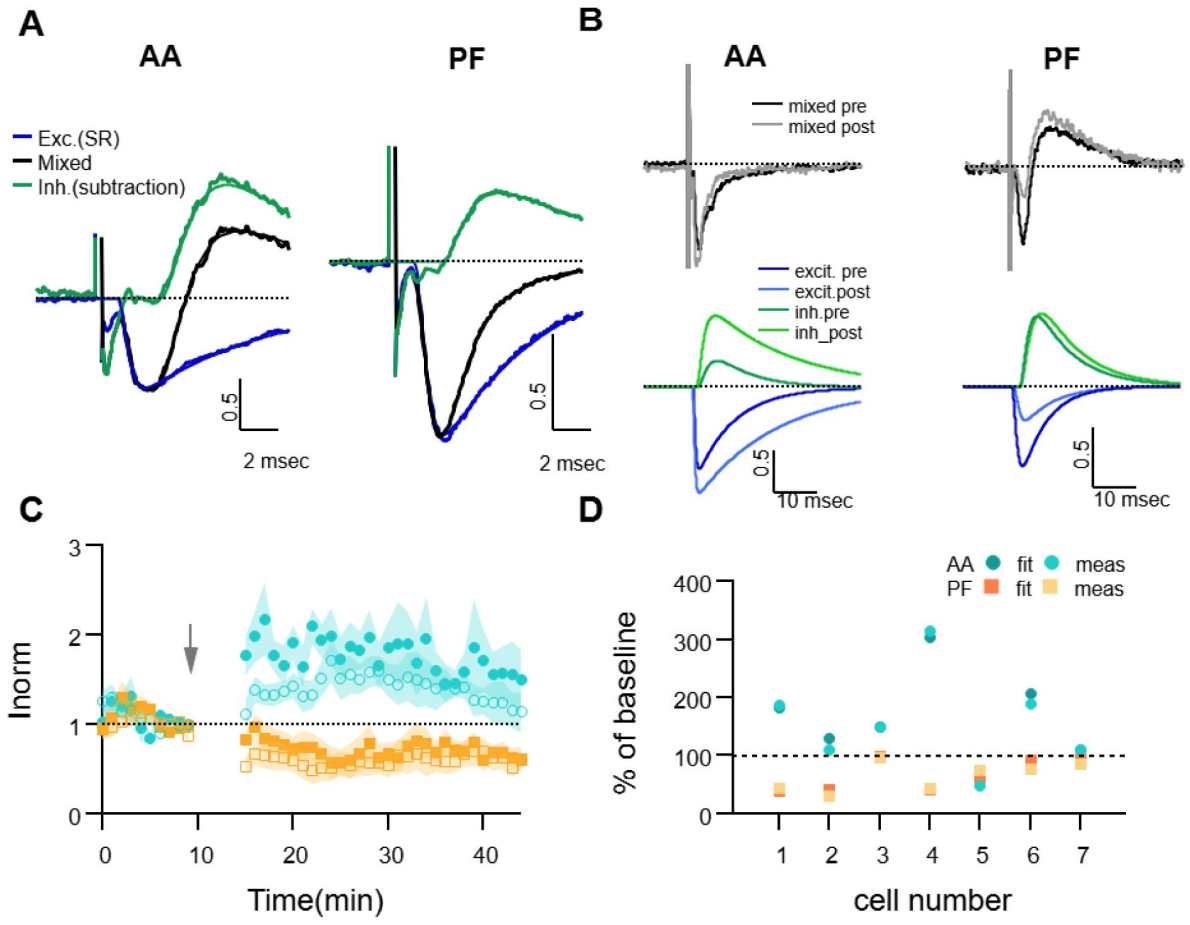

Supplementary Figure 3

Dissecting excitation and inhibition shows that EPSC amplitude and long term changes are well estimated with the direct measure method.

A. Fitting procedure used to extract the excitatory and inhibitory components of the recorded mixed PSCs (EPSC + IPSC). Traces recorded during the baseline period were normalised to the peak excitatory response and then averaged over all cells. The mixed evoked PSC (black thick line) is shown together with the excitatory response recorded during SR application (blue thick line). The inhibitory trace (green thick line) is the difference between the mixed PSC and the fit of the excitatory response. The EPSC and IPSC fitting functions as well as the mixed fitting function resulting from the sum of the two are overlaid (thinner lines, same colour), showing good agreement with the data. On average, inhibition was delayed and relatively smaller than excitation for both AA and PF pathways. **B** Sample traces for an experiment where the excitatory and inhibitory components were extracted from the mixed PSC for both the baseline and 25-30 mins after induction; top: mixed PSCs for AA (left) and PF (right) before and after induction; below are the corresponding excitatory (blue, dark and light for pre and post-induction respectively) and inhibitory components (green, dark and light for pre and post-induction respectively). The AA-EPSC increased and the PF-EPSC decreased, while both AA- and PF-IPSCs increased in this example. **C.** Average time course of the EPSCs relative amplitude (measured with the standard minimum amplitude method) for 7 experiments in which gabazine (SR) was applied transiently 20 min before and 30 min after LTP induction. Peak EPSCs amplitudes of the first and second evoked responses in the pair for both AA (blue, closed circles: first response in the pair, open circles: second response) and PF(orange, closed squares: first response in the pair, open squares: second response) stimulation. Short and long term plastic changes are not different from control experiments. **D.** The normalised EPSC amplitude 25-30 mins after induction is compared for the two analysis methods for each cell, either measured directly as the minimum of the recorded response (meas) or that of the excitatory fitting function (fit). Disynaptic inhibition only slightly affected the measure of the real excitatory peak, both for AA- (blue triangles) and PF-EPSC(orange circles) (AA measured:160 ± 30 %, from fit: 160 ± 30% and PF measured: 65 ± 9 %, from fit: 70 ± 10 %).

References

Aiba A., Kano M., Chen C., Stanton M. E., Fox G. D., Herrup K., Zwingman T. A., Tonegawa S (1994) **Deficient cerebellar long-term depression and impaired motor learning in mGluR1 mutant mice** *Cell* **79**:377–388

Albus JS (1971) **A theory of cerebellar function** *Mathematical Biosciences* **10**:25–61 https://doi.org/10.1016/0025-5564(71)90051-4

Astorga G., Bao J., Marty A., Augustine G. J., Franconville R., Jalil A., Bradley J., Llano I (2015) **An excitatory GABA loop operating in vivo** *Frontiers in Cellular Neuroscience* **9** https://doi.org/10.3389/fncel.2015.00275

Berglund K., Wen L., Dunbar R. L., Feng G., Augustine G. J (2016) **Optogenetic Visualization of Presynaptic Tonic Inhibition of Cerebellar Parallel Fibers** *The Journal of Neuroscience: The Official Journal of the Society for Neuroscience* **36**:5709–5723 https://doi.org/10.1523/JNEUROSCI.4366-15.2016

Bidoret C., Ayon A., Barbour B., Casado M (2009) **Presynaptic NR2A-containing NMDA receptors implement a high-pass filter synaptic plasticity rule** *Proceedings of the National Academy of Sciences of the United States of America* **106**:14126–14131 https://doi.org/10.1073/pnas.0904284106

Bidoret C., Bouvier G., Ayon A., Szapiro G., Casado M (2015) **Properties and molecular identity of NMDA receptors at synaptic and non-synaptic inputs in cerebellar molecular layer interneurons** *Frontiers in Synaptic Neuroscience* **7** https://doi.org/10.3389/fnsyn.2015.00001

Binda F., Dorgans K., Reibel S., Sakimura K., Kano M., Poulain B., Isope P (2016) **Inhibition promotes long-term potentiation at cerebellar excitatory synapses** *Scientific Reports* **6** https://doi.org/10.1038/srep33561

Brown S. P., Brenowitz S. D., Regehr W. G (2003) **Brief presynaptic bursts evoke synapse-specific retrograde inhibition mediated by endogenous cannabinoids** *Nature Neuroscience* **6**:1048–1057 https://doi.org/10.1038/nn1126

Bouvier G., Higgins D., Spolidoro M., Carrel D., Mathieu B., Léna C., Dieudonné S., Barbour B., Brunel N., Casado M (2016) **Burst-Dependent Bidirectional Plasticity in the Cerebellum Is Driven by Presynaptic NMDA Receptors** *Cell Reports* **15**:104–116 https://doi.org/10.1016/j.celrep.2016.03.004

Canepari M., Auger C., Ogden D (2004) **Ca2+ ion permeability and single-channel properties of the metabotropic slow EPSC of rat Purkinje neurons** *The Journal of Neuroscience: The Official Journal of the Society for Neuroscience* **24**:3563–3573 https://doi.org/10.1523/JNEUROSCI.5374-03.2004

Canepari M., Ogden D (2006) **Kinetic, pharmacological and activity-dependent separation of two Ca2+ signalling pathways mediated by type 1 metabotropic glutamate receptors in rat Purkinje neurones** *The Journal of Physiology* **573**:65–82 https://doi.org/10.1113/jphysiol.2005.103770

Carey M. R., Myoga M. H., McDaniels K. R., Marsicano G., Lutz B., Mackie K., Regehr W. G (2011) **Presynaptic CB1 receptors regulate synaptic plasticity at cerebellar parallel fiber synapses** *Journal of Neurophysiology* **105**:958–963 https://doi.org/10.1152/jn.00980.2010

Casado M., Isope P., Ascher P (2002) **Involvement of presynaptic N-methyl-D-aspartate receptors in cerebellar long-term depression** *Neuron* **33**:123–130 https://doi.org/10.1016/s0896-6273(01)00568-2

Chavas J., Marty A (2003) **Coexistence of excitatory and inhibitory GABA synapses in the cerebellar interneuron network** *The Journal of Neuroscience: The Official Journal of the Society for Neuroscience* **23**:2019–2031

Coesmans M., Weber J. T., De Zeeuw C. I., Hansel C. (2004) **Bidirectional parallel fiber plasticity in the cerebellum under climbing fiber control** *Neuron* **44**:691–700 https://doi.org/10.1016/j.neuron.2004.10.031

Cohen D., Yarom Y (1998) **Patches of synchronized activity in the cerebellar cortex evoked by mossy-fiber stimulation: Questioning the role of parallel fibers** *Proceedings of the National Academy of Sciences of the United States of America* **95**:15032–15036 https://doi.org/10.1073/pnas.95.25.15032

Daniel H., Hemart N., Jaillard D., Crepel F (1992) **Coactivation of metabotropic glutamate receptors and of voltage-gated calcium channels induces long-term depression in cerebellar Purkinje cells in vitro** *Experimental Brain Research* **90**:327–331 https://doi.org/10.1007/BF00227245

Devi S. P. S., Howe J. R., Auger C (2016) **Train stimulation of parallel fibre to Purkinje cell inputs reveals two populations of synaptic responses with different receptor signatures** *The Journal of Physiology* **594**:3705–3727 https://doi.org/10.1113/JP272415

Duguid I. C., Smart T. G (2004) **Retrograde activation of presynaptic NMDA receptors enhances GABA release at cerebellar interneuron-Purkinje cell synapses** *Nature Neuroscience* **7**:525–533 https://doi.org/10.1038/nn1227

Ekerot C. F., Jörntell H (2001) **Parallel fibre receptive fields of Purkinje cells and interneurons are climbing fibre-specific** *The European Journal of Neuroscience* **13**:1303–1310 https://doi.org/10.1046/j.0953-816x.2001.01499.x

Finch E. A., Augustine G. J (1998) **Local calcium signalling by inositol-1,4,5-trisphosphate in Purkinje cell dendrites** *Nature* **396**:753–756 https://doi.org/10.1038/25541

Glitsch M., Marty A (1999) **Presynaptic effects of NMDA in cerebellar Purkinje cells and interneurons** *The Journal of Neuroscience: The Official Journal of the Society for Neuroscience* **19**:511–519 https://doi.org/10.1523/JNEUROSCI.19-02-00511.1999

González-Calvo I. *et al.* (2021) **Sushi domain-containing protein 4 controls synaptic plasticity and motor learning** *ELife* **10** https://doi.org/10.7554/eLife.65712

Hémart N., Daniel H., Jaillard D., Crépel F (1995) **Receptors and second messengers involved in long-term depression in rat cerebellar slices in vitro: A reappraisal** *The European Journal of Neuroscience* **7**:45–53 https://doi.org/10.1111/j.1460-9568.1995.tb01019.x

Hildebrand M. E. *et al.* (2009) **Functional coupling between mGluR1 and Cav3.1 T-type calcium channels contributes to parallel fiber-induced fast calcium signaling within Purkinje cell dendritic spines** *The Journal of Neuroscience: The Official Journal of the Society for Neuroscience* **29**:9668–9682 https://doi.org/10.1523/JNEUROSCI.0362-09.2009

Ichikawa R., Hashimoto K., Miyazaki T., Uchigashima M., Yamasaki M., Aiba A., Kano M., Watanabe M (2016) **Territories of heterologous inputs onto Purkinje cell dendrites are segregated by mGluR1-dependent parallel fiber synapse elimination** *Proceedings of the National Academy of Sciences of the United States of America* **113**:2282–2287 https://doi.org/10.1073/pnas.1511513113

Isope P., Barbour B (2002) **Properties of unitary granule cell—>Purkinje cell synapses in adult rat cerebellar slices** *The Journal of Neuroscience: The Official Journal of the Society for Neuroscience* **22**:9668–9678 https://doi.org/10.1523/JNEUROSCI.22-22-09668.2002

Ito M., Kano M (1982) **Long-lasting depression of parallel fiber-Purkinje cell transmission induced by conjunctive stimulation of parallel fibers and climbing fibers in the cerebellar cortex** *Neuroscience Letters* **33**:253–258 https://doi.org/10.1016/0304-3940(82)90380-9

Jörntell H., Ekerot C.-F (2002) **Reciprocal bidirectional plasticity of parallel fiber receptive fields in cerebellar Purkinje cells and their afferent interneurons** *Neuron* **34**:797–806 https://doi.org/10.1016/s0896-6273(02)00713-4

Konnerth A., Dreessen J., Augustine G. J (1992) **Brief dendritic calcium signals initiate long-lasting synaptic depression in cerebellar Purkinje cells** *Proceedings of the National Academy of Sciences of the United States of America* **89**:7051–7055 https://doi.org/10.1073/pnas.89.15.7051

Kono M., Kakegawa W., Yoshida K., Yuzaki M (2019) **Interneuronal NMDA receptors regulate long-term depression and motor learning in the cerebellum** *The Journal of Physiology* **597**:903–920 https://doi.org/10.1113/JP276794

Kostadinov D., Beau M., Blanco-Pozo M., Häusser M (2019) **Predictive and reactive reward signals conveyed by climbing fiber inputs to cerebellar Purkinje cells** *Nature Neuroscience* **22**:950–962 https://doi.org/10.1038/s41593-019-0381-8

Lev-Ram V., Jiang T., Wood J., Lawrence D. S., Tsien R. Y (1997) **Synergies and coincidence requirements between NO, cGMP, and Ca2+ in the induction of cerebellar long-term depression** *Neuron* **18**:1025–1038 https://doi.org/10.1016/s0896-6273(00)80340-2

Llano I., Marty A., Armstrong C. M., Konnerth A (1991) **Synaptic- and agonist-induced excitatory currents of Purkinje cells in rat cerebellar slices** *The Journal of Physiology* **434**:183–213 https://doi.org/10.1113/jphysiol.1991.sp018465

Lu H., Esquivel A. V., Bower J. M (2009) **3D electron microscopic reconstruction of segments of rat cerebellar Purkinje cell dendrites receiving ascending and parallel fiber granule cell synaptic inputs** *The Journal of Comparative Neurology* **514**:583–594 https://doi.org/10.1002/cne.22041

Maejima T., Hashimoto K., Yoshida T., Aiba A., Kano M (2001) **Presynaptic inhibition caused by retrograde signal from metabotropic glutamate to cannabinoid receptors** *Neuron* **31**:463–475 https://doi.org/10.1016/s0896-6273(01)00375-0

Marcaggi P., Attwell D (2005) **Endocannabinoid signaling depends on the spatial pattern of synapse activation** *Nature Neuroscience* **8**:776–781 https://doi.org/10.1038/nn1458

Marr D (1969) **A theory of cerebellar cortex** *The Journal of Physiology* **202**:437–470 https://doi.org/10.1113/jphysiol.1969.sp008820

Medina J. F., Lisberger S. G (2008) **Links from complex spikes to local plasticity and motor learning in the cerebellum of awake-behaving monkeys** *Nature Neuroscience* **11**:1185–1192 https://doi.org/10.1038/nn.2197

Montgomery J. C., Bodznick D (1994) **An adaptive filter that cancels self-induced noise in the electrosensory and lateral line mechanosensory systems of fish** *Neuroscience Letters* **174**:145–148 https://doi.org/10.1016/0304-3940(94)90007-8

Nakao H., Kishimoto Y., Hashimoto K., Kitamura K., Yamasaki M., Nakao K., Watanabe M., Kano M., Kirino Y., Aiba A (2019) **MGluR1 in cerebellar Purkinje cells is essential for the formation but not expression of associative eyeblink memory** *Scientific Reports* **9** https://doi.org/10.1038/s41598-019-43744-z

Napper R. M., Harvey R. J (1988) **Number of parallel fiber synapses on an individual Purkinje cell in the cerebellum of the rat** *The Journal of Comparative Neurology* **274**:168–177 https://doi.org/10.1002/cne.902740204

Otsu Y. *et al.* (2014) **Activity-dependent gating of calcium spikes by A-type K+ channels controls climbing fiber signaling in Purkinje cell dendrites** *Neuron* **84**:137–151 https://doi.org/10.1016/j.neuron.2014.08.035

Pichitpornchai C., Rawson J. A., Rees S (1994) **Morphology of parallel fibres in the cerebellar cortex of the rat: An experimental light and electron microscopic study with biocytin** *The Journal of Comparative Neurology* **342**:206–220 https://doi.org/10.1002/cne.903420205

Piochon C., Irinopoulou T., Brusciano D., Bailly Y., Mariani J., Levenes C (2007) **NMDA receptor contribution to the climbing fiber response in the adult mouse Purkinje cell** *The Journal of Neuroscience: The Official Journal of the Society for Neuroscience* **27**:10797–10809 https://doi.org/10.1523/JNEUROSCI.2422-07.2007

Piochon C., Titley H. K., Simmons D. H., Grasselli G., Elgersma Y., Hansel C (2016) **Calcium threshold shift enables frequency-independent control of plasticity by an instructive signal** *Proceedings of the National Academy of Sciences of the United States of America* **113**:13221–13226 https://doi.org/10.1073/pnas.1613897113

Rowan M. J. M., Bonnan A., Zhang K., Amat S. B., Kikuchi C., Taniguchi H., Augustine G. J., Christie J. M (2018) **Graded Control of Climbing-Fiber-Mediated Plasticity and Learning by Inhibition in the Cerebellum** *Neuron* **99**:999–1015 https://doi.org/10.1016/j.neuron.2018.07.024

Safo P. K., Regehr W. G (2005) **Endocannabinoids control the induction of cerebellar LTD** *Neuron* **48**:647–659 https://doi.org/10.1016/j.neuron.2005.09.020

Safo P., Regehr W. G (2008) **Timing dependence of the induction of cerebellar LTD** *Neuropharmacology* **54**:213–218 https://doi.org/10.1016/j.neuropharm.2007.05.029

Sawtell N. B (2017) **Neural Mechanisms for Predicting the Sensory Consequences of Behavior: Insights from Electrosensory Systems** *Annual Review of Physiology* **79**:381–399 https://doi.org/10.1146/annurev-physiol-021115-105003

Schmahmann J. D., Sherman J. C (1998) **The cerebellar cognitive affective syndrome** *Brain: A Journal of Neurology* **121**:561–579 https://doi.org/10.1093/brain/121.4.561

Schonewille M., Girasole A. E., Rostaing P., Mailhes-Hamon C., Ayon A., Nelson A. B., Triller A., Casado M., De Zeeuw C. I., Bouvier G. (2021) **NMDARs in granule cells contribute to parallel fiber-Purkinje cell synaptic plasticity and motor learning** *Proceedings of the National Academy of Sciences of the United States of America* **118** https://doi.org/10.1073/pnas.2102635118

Sims R. E., Hartell N. A (2005) **Differences in transmission properties and susceptibility to long-term depression reveal functional specialization of ascending axon and parallel fiber synapses to Purkinje cells** *The Journal of Neuroscience: The Official Journal of the Society for Neuroscience* **25**:3246–3257 https://doi.org/10.1523/JNEUROSCI.0073-05.2005

Sims R. E., Hartell N. A (2006) **Differential susceptibility to synaptic plasticity reveals a functional specialization of ascending axon and parallel fiber synapses to cerebellar Purkinje cells** *The Journal of Neuroscience: The Official Journal of the Society for Neuroscience* **26**:5153–5159 https://doi.org/10.1523/JNEUROSCI.4121-05.2006

Stell B. M., Rostaing P., Triller A., Marty A (2007) **Activation of presynaptic GABA(A) receptors induces glutamate release from parallel fiber synapses** *The Journal of Neuroscience: The Official Journal of the Society for Neuroscience* **27**:9022–9031 https://doi.org/10.1523/JNEUROSCI.1954-07.2007

Stoodley C. J., Schmahmann J. D (2010) **Evidence for topographic organization in the cerebellum of motor control versus cognitive and affective processing** *Cortex; a Journal Devoted to the Study of the Nervous System and Behavior* **46**:831–844 https://doi.org/10.1016/j.cortex.2009.11.008

Takechi H., Eilers J., Konnerth A (1998) **A new class of synaptic response involving calcium release in dendritic spines** *Nature* **396**:757–760 https://doi.org/10.1038/25547

Wagner M. J., Kim T. H., Savall J., Schnitzer M. J., Luo L (2017) **Cerebellar granule cells encode the expectation of reward** *Nature* **544**:96–100 https://doi.org/10.1038/nature21726

Walter J. T., Dizon M.-J., Khodakhah K (2009) **The functional equivalence of ascending and parallel fiber inputs in cerebellar computation** *The Journal of Neuroscience: The Official Journal of the Society for Neuroscience* **29**:8462–8473 https://doi.org/10.1523/JNEUROSCI.5718-08.2009

Yang Y., Lisberger S. G (2014) **Purkinje-cell plasticity and cerebellar motor learning are graded by complex-spike duration** *Nature* **510**:529–532 https://doi.org/10.1038/nature13282

Zucker R. S., Regehr W. G (2002) **Short-term synaptic plasticity** *Annual Review of Physiology* **64**:355–405 https://doi.org/10.1146/annurev.physiol.64.092501.114547

Editors

Reviewing Editor
Aya Ito-Ishida
RIKEN Center for Brain Science, Saitama, Japan

Senior Editor
Lu Chen
Stanford University, Stanford, United States of America

Reviewer #1 (Public Review):

In this study, the authors address a fundamental unresolved question in cerebellar physiology: do synapses between granule cells (GCs) and Purkinje cells (PCs) made by the ascending part of the axon (AA) have different synaptic properties to those made by parallel fibers? This is an important question because GCs integrate sensorimotor information from many brain areas with a precise and complex topography.

The authors argue that GCs located close to the PCs essentially contact PC dendrites through the ascending part of their axon. They demonstrate that high-frequency (100 Hz) joint stimulation of distant parallel fibers and local GCs potentiates AA-PC synapses, while parallel fiber-PC synapses are depressed. On the basis of paired pulse ratio analysis, they concluded that evoked plasticity was postsynaptic. When individual pathways are stimulated alone, no LTP is observed. This associative plasticity appears to be sensitive to timing, as stimulation of parallel fibers first results in depression, while stimulation of the AA pathway has no effect. NMDA, mGluR1 and GABAA receptors are involved in this plasticity.

Overall, associative modulation of synaptic transmission is convincing, and the experiments carried out support this conclusion.

One of its weaknesses is that it contradicts the numerous experiments conducted by many groups that have studied plasticity at this connection (e.g. Bouvier et al 2016, Piochon et al 2016, Binda et al, 2016, Schonewille et al 2021). According to the literature, high-frequency stimulation of parallel fibers leads to postsynaptic potentiation under many different experimental conditions (blocked or unblocked inhibition, stimulation protocols, internal solution composition). This discrepancy was not investigated experimentally.

Another weakness is the lack of evidence that AAs have been stimulated. Indeed, without filling the PC with fluorescent dye or biocytin during the experiment, and without reconstructing the anatomical organization, it is difficult to assess whether the stimulating pipette is actually positioned in the GC cluster that potentially contacts the PC with AAs. Although the idea that AAs repeatedly contact the same Purkinje cell has been propagated, to the reviewer's knowledge, no direct demonstration of this hypothesis has yet been published. In fact, what has been demonstrated (Walter et al 2009; Spaeth et al 2022) is that GCs have a higher probability of being connected to nearby PCs, but not necessarily associated with AAs.

https://doi.org/10.7554/eLife.96140.2.sa3

Reviewer #2 (Public Review):

Summary:

The authors describe a form of synaptic plasticity at synapses from granule cells onto Purkinje cells in the mouse cerebellum, which is specific to synapses from granule cells close

to the cell body but not to distal ones. This plasticity is induced by the paired or associative stimulation of the two types of synapses because it is not observed with stimulation of one type of synapse alone. In addition, this form of plasticity is dependent on the order in which the stimuli are presented and is dependent on NMDA receptors, metabotropic glutamate receptors and to some degree on GABAA receptors.

Strengths:

The focus of the authors on the properties of two different synapse-types on cerebellar Purkinje cells is interesting and relevant, given previous results that ascending and parallel fiber synapses might be functionally different and undergo different forms of plasticity (although it hasn't been proven here that the two types of synapses are indeed ascending vs parallel fiber synapses). Nevertheless, the interaction between proximal vs. distal stimulation driven synapse types during plasticity is important for understanding cerebellar function. The demonstration of timing and order-dependent potentiation of only one pathway, and not another, after associative stimulation of both pathways, changes our understanding of potential plasticity mechanisms. In addition, this observation opens up many new questions on underlying intracellular mechanisms as well as on its relevance for cerebellar learning.

Weaknesses:

A concern with this study is that all recordings demonstrate "rundown", a progressive decrease in the amplitude of the EPSC, starting during the baseline period and continuing after the plasticity-induction stimulus. The issues that are causing rundown are not known and may or may not be related to the cellular processes involved in synaptic plasticity. This concern applies in particular to all the experiments where there is a decrease in synaptic strength. However, a key finding of this paper is the associative potentiation of one pathway, which is clearly different from all conditions where there is a decrease in synaptic strength and raises confidence in the authors' conclusions.

In addition, there is some inconsistency with previous results; specifically, that no PF-LTP was induced by PF-alone repeated stimulation.

It remains for future work to identify what these two synapse types, distinguished by the stimulation location, actually are, and where they are on the Purkinje cell dendritic tree. What this specific timing rule is important for is also something that remains to be discovered. Its potential relevance for plasticity and learning will depend on what information these AA vs PF synapses carry, and why their association is meaningful for the circuit and for a behavior. Overall, this study opens up many new questions for the field.

https://doi.org/10.7554/eLife.96140.2.sa2

Reviewer #3 (Public Review):

Summary:

Granule cells' axons bifurcate to form parallel fibers (PFs) and ascending axons (AAs). While the significance of PFs on cerebellar plasticity is widely acknowledged, the importance of AAs remains unclear. In the current paper, Conti and Auger conducted electrophysiological experiments in rat cerebellar slices and identified a new form of synaptic plasticity in the AA-Purkinje cell (PC) synapses.

Strengths:

The authors applied simultaneous stimulation of AAs and PFs and recorded from PCs and discovered that the strength of AA-PC synapses and PF-PC synapses change in opposite

directions: while AA-PC EPSCs increased, PFs-EPSCs decreased. This finding suggests that synaptic responses to AAs and PFs in PCs are jointly regulated, working as an additional mechanism to integrate motor/sensory input. The existence of such plasticity mechanisms may offer new perspectives in studying and modeling cerebellum-dependent behavior. Overall, the experiments are performed well.

Weaknesses:

There are two weaknesses. First, the baseline of electrophysiological recordings is influenced significantly by run-down, limiting the interpretability of the data. Because the amplitude of AA-EPSCs is relatively small, the run-down may have masked some of the changes in EPSCs. However, the authors managed this difficulty using appropriate controls and statistical analysis. Second, while the authors show AA-LTP depends on mGluR, NMDA receptors, and GABA-A receptors, which cell types express these receptors and how they contribute to plasticity is not clarified. Cell-type-specific knockdown of these receptors may clarify this point in future studies.

https://doi.org/10.7554/eLife.96140.2.sa1

Author response:

The following is the authors' response to the original reviews.

> ***Public Reviews:***
>
> ***Reviewer #1 (Public Review):***
>
> *In this study, the authors address a fundamental unresolved question in cerebellar physiology: do synapses between granule cells (GCs) and Purkinje cells (PCs) made by the ascending part of the axon (AA) have different synaptic properties from those made by parallel fibers? This is an important question, as GCs integrate sensorimotor information from numerous brain areas with a precise and complex topography.*
>
> *Summary:*
>
> *The authors argue that CGs located close to PCs essentially contact PC dendrites via the ascending part of their axons. They demonstrate that joint high-frequency (100 Hz) stimulation of distant parallel fibers and local CGs potentiates AA-PC synapses, while parallel fiber-PC synapses are depressed. On the basis of paired-pulse ratio analysis, they concluded that evoked plasticity was postsynaptic. When individual pathways were stimulated alone, no LRP was observed. This associative plasticity appears to be sensitive to timing, as stimulation of parallel fibers first results in depression, while stimulation of the AA pathway has no effect. NMDA, mGluR1 and GABAA receptors are involved in this plasticity.*
>
> *Strengths:*
>
> *Overall, the associative modulation of synaptic transmission is convincing, and the experiments carried out support this conclusion. However, weaknesses limit the scope of the results.*
>
> *Weaknesses:*
>
> *One of the main weaknesses of this study is the suggestion that high-frequency parallel-fiber stimulation cannot induce long term potentiation unless combined with AA stimulation. Although we acknowledge that the stimulation and recording conditions were different from those of other studies, according to the literature (e.g. Bouvier et al*

> *2016, Piochon et al 2016, Binda et al, 2016, Schonewille et al 2021 and others), high-frequency stimulation of parallel fibers leads to long-term postsynaptic potentiation under many different experimental conditions (blocked or unblocked inhibition, stimulation protocols, internal solution composition). Furthermore, in vivo experiments have confirmed that high-frequency parallel fibers are likely to induce long-term potentiation (Jorntell and Ekerot, 2002; Wang et al, 2009).*
>
> *This article provides further evidence that long-term plasticity (LTP and LTD) at this connection is a complex and subtle mechanism underpinned by many different transduction pathways. It would therefore have been interesting to test different protocols or conditions to explain the discrepancies observed in this dataset.*

Even though this is not the main result of this study, we acknowledge that the control experiments done on PF stimulation add a puzzling result to an already contradictory literature. High frequency parallel fibre stimulation (in isolation) has been shown to induce long term potentiation in vitro, but not always, and most importantly, this has been shown in vivo. This was the reason for choosing that particular stimulation protocol. Examination of in vitro studies, however, show that the results are variable and even contradictory. Most were done in the presence of GABAA receptor antagonists, including the SK channel blocker Bicuculline, whereas in the study by Binda (2016), LTP was blocked by GABAA receptor inhibition. In some studies also, LTP was under the control of NMDAR activation only, whereas in Binda (2016), it was under the control of mGluR activation. Moreover, most experiments were done in mice, whereas our study was done in rats. Our results reveal multiple mechanisms working together to produce plasticity, which are highly sensitive to in vitro conditions. We designed our experiments to be close to the physiological conditions, with inhibition preserved and a physiological chloride gradient. It is likely that experimental differences have given rise to the variability of the results and our inability to reproduce PF-LTP, but it was not the aim of this study to dissect the subtleties of the different experimental protocols and models.

We have modified the Discussion to cover that point fully.

> *Another important weakness is the lack of evidence that the AAs were stimulated. Indeed, without filling the PC with fluorescent dye or biocytin during the experiment, and without reconstructing the anatomical organization, it is difficult to assess whether the stimulating pipette is positioned in the GC cluster that is potentially in contact with the PC with the AAs. According to EM microscopy, AAs account for 3% of the total number of synapses in a PC, which could represent a significant number of synapses. Although the idea that AAs repeatedly contact the same Purkinje cell has been propagated, to the best of the review author's knowledge, no direct demonstration of this hypothesis has yet been published. In fact, what has been demonstrated (Walter et al 2009; Spaeth et al 2022) is that GCs have a higher probability of being connected to nearby PCs, but are not necessarily associated with AAs.*

We fully agree with the reviewer that we have not identified morphologically ascending axon synapses, and we stress this fact both in the first paragraph of the Results section, and again at the beginning of Discussion. Our point is mainly topographical, given the well documented geometrical organisation of the cerebellar cortex. Strictly speaking, inputs are local (including AAs) or distal (PFs). Similarly, the studies by Isope and Barbour (2002) and Walter et al. (2009), just like Sims and Hartell (2005 and 2006), have coined the term ‘ascending axon’ when drawing conclusions about locally stimulated inputs. Moreover, our results do not rely on or assume multiple contacts, stronger connections, or higher probability of connections between ascending axons and Purkinje cells. Our results only demonstrate a different plasticity outcome for the two types of inputs. Therefore, our manuscript could be rephrased with the terms ‘local’ and ‘distal’ granule cell inputs, but this would have no more implication

for the results or the computation performed in Purkinje cells. However, in our experience, these terms are more confusing, and consistent with the literature, we do not wish to make this modification. However, we have modified the abstract of the manuscript to clarify this point.

> ***Reviewer #2 (Public Review):***
>
> *Summary:*
>
> *The authors describe a form of synaptic plasticity at synapses from granule cells onto Purkinje cells in the mouse cerebellum, which is specific to synapses proximal to the cell body but not to distal ones. This plasticity is induced by the paired or associative stimulation of the two types of synapses because it is not observed with stimulation of one type of synapse alone. In addition, this form of plasticity is dependent on the order in which the stimuli are presented, and is dependent on NMDA receptors, metabotropic glutamate receptors and to some degree on GABAA receptors. However, under all experimental conditions described, there is a progressive weakening or run-down of synaptic strength. Therefore, plasticity is not relative to a stable baseline, but relative to a process of continuous decline that occurs whether or not there is any plasticity-inducing stimulus.*

As highlighted by the reviewer, we observed a postsynaptic rundown of the EPSC amplitude for both input pathways. Rundown could be mistaken for a depression of synaptic currents, not for a potentiation, and the progressive decrease of the EPSC amplitude during the course of an experiment leads to an underestimate of the absolute potentiation. We have taken the view to provide a strong set of control data rather than selecting experiments based on subjective criteria or applying a cosmetic compensation procedure. We have conducted control experiments with no induction (n = 17), which give a good indication of the speed and amplitude of the rundown. Comparison shows a highly significant potentiation of the ascending axon EPSC. Depression of the parallel fibre EPSC, on the other hand, was not significantly different from rundown, and we have not spoken of parallel fibre long term depression. The data show thus very clearly that ascending axon and parallel fibre synapses behave differently following the costimulation protocol.

> *Strengths:*
>
> *The focus of the authors on the properties of two different synapse-types on cerebellar Purkinje cells is interesting and relevant, given previous results that ascending and parallel fiber synapses might be functionally different and undergo different forms of plasticity. In addition, the interaction between these two synapse types during plasticity is important for understanding cerebellar function. The demonstration of timing and order-dependent potentiation of only one pathway, and not another, after associative stimulation of both pathways, changes our understanding of potential plasticity mechanisms. In addition, this observation opens up many new questions on underlying intracellular mechanisms as well as on its relevance for cerebellar learning and adaptation.*
>
> *Weaknesses and suggested improvements:*
>
> *A concern with this study is that all recordings demonstrate "rundown", a progressive decrease in the amplitude of the EPSC, starting during the baseline period and continuing after the plasticity-induction stimulus. In the absence of a stable baseline, it is hard to know what changes in strength actually occur at any set of synapses. Moreover, the issues that are causing rundown are not known and may or may not be related to the cellular processes involved in synaptic plasticity. This concern applies in particular to all the experiments where there is a decrease in synaptic strength.*

We have provided an answer to that point directly below the summary paragraph. We will just add here that if the phenomenon causing rundown was involved in plasticity, it should affect plasticity of both inputs, which was not the case, clearly distinguishing the ascending axon and parallel fibre inputs.

> *The authors should consider changes in the shape of the EPSC after plasticity induction, as in Fig 1 (orange trace) as this could change the interpretation.*

Figure 1 shows an average response composed of evoked excitatory and inhibitory synaptic currents. The third section of Supplementary material (supplementary figure 3) shows that this complex shape is given by an EPSC followed by a delayed disynaptic IPSC. We would like to point out that while separating EPSC from IPSC might appear difficult from average traces due to the averaged jitter in the onset of the synaptic currents, boundaries are much clearer when analysing individual traces. In the same section we discuss the results of experiments in which transient applications of SR 95531 before and after the induction protocol allowed us to measure the EPSC, while maintaining the same experimental conditions during induction. Analysis of the kinetics of the EPSCs during SR application at the beginning and end of experiments, showed that there is no change in the time to peak of both AA and PF response. The decay time of AA- and PF-EPSCs are slightly longer at the end of the experiment, even if the difference is not significant for AA inputs. This analysis has been added to the Supplementary material. Our analysis, that uses as template the EPSCs kinetics measured at the beginning and at the end of the experiments, takes directly into account these changes. The results show clearly that the presence of disynaptic inhibition doesn't significantly affect the measure of the peak EPSC after the induction protocol nor the estimate of plasticity.

In addition, the inconsistency with previous results is surprising and is not explained; specifically, that no PF-LTP was induced by PF-alone repeated stimulation.

In our experimental conditions, PF-LTP was not induced when stimulating PF only, the condition that reproduces experiments in the literature. As discussed in our response to reviewer 1, a close look at the literature, however, reveals variabilities and contradictions behind seemingly similar results. They reveal intricate mechanisms working together to produce plasticity, which are sensitive to in vitro conditions. We designed our experiments to be close to physiological conditions, with inhibition preserved and a physiological chloride gradient. It is likely that experimental differences have given rise to the variability of the results and our inability to observe PF-LTP. We have modified the Discussion section to cover that point thoroughly in the context of past results.

> *The authors test the role of NMDARs, GABAARs and mGluRs in the phenotype they describe. The data suggest that the form of plasticity described here is dependent on any one of the three receptors. However, the location of these receptors varies between the Purkinje cells, granule cells and interneurons. The authors do not describe a convincing hypothetical model in which this dependence can be explained. They suggest that there is crosstalk between AA and PF synapses via endocannabinoids downstream of mGluR or NO downstream of NMDARs. However, it is not clear how this could lead to the long-term potentiation that they describe. Also, there is no long-lasting change in paired-pulse ratio, suggesting an absence of changes in presynaptic release.*

We suggest in the result section that the transient change in paired pulse ratio (PPR) is linked to a transient presynaptic effect, but there was no significant long term change of the PPR, suggesting that the long term effects observed are linked to postsynaptic changes. We now stress this point in the Results and Discussion sections.

Concerning the involvement of multiple molecular pathways, investigators often tested for the involvement of NMDAR or mGluRs in cerebellar plasticity, rarely both. Here we showed that both pathways are involved. The conjunctive requirement for NMDAR and mGluR activation could easily be explained based on the dependence of cerebellar LTP and LTD on the concentrations of both NO and postsynaptic calcium (Coesman et al., 2004; Safo and Regehr, 2005; Bouvier et al., 2016; Piochon et al., 2016).

We also observed an effect of GABAergic inhibition. GABAergic inhibition was elegantly shown by Binda (2016) to regulate calcium entry together with mGluRs, and control plasticity induction. A similar mechanism could contribute to our results, although inhibition might have additional effects. We have modified the Discussion of the manuscript to clarify the pathways involved in plasticity and added a diagram to highlight the links between the different molecular pathways, potential cross talk mechanisms, and the location of receptors.

> *Is the synapse that undergoes plasticity correctly identified? In this study, since GABAergic inhibition is not blocked for most experiments, PF stimulation can result in both a direct EPSC onto the Purkinje cell and a disynaptic feedforward IPSC. The authors do address this issue with Supplementary Fig 3, where the impact of the IPSC on the EPSC within the EPSC/IPSC sequence is calculated. However, a change in waveform would complicate this analysis. An experiment with pharmacological blockade will make the interpretation more robust. The observed dependence of the plasticity on GABAA receptors is an added point in favor of the suggested additional experiments.*

We did consider that due to long recording times there might be kinetic changes, and that's the reason why the experiments of Supplementary figure 3 were done with pharmacological blockade of GABAAR with SR, both before and again after LTP induction. The estimate of the amplitude of the EPSC is based on the actual kinetics of the response at both times.

> *A primary hypothesis of this study is that proximal, or AA, and distal, or PF, synapses are different and that their association is specifically what drives plasticity. The alternative hypothesis is that the two synapse-types are the same. Therefore, a good control for pairing AA with PF would be to pair AA with AA and PF with PF, thereby demonstrating that pairing with each other is different from pairing with self.*

Pairing AA with AA would be difficult because stimulation of AA can only be made from a narrow band below the PC and we would likely end up stimulating overlapping sets of synapses. However, Figure 5 shows the effect of stimulating PF and PF, while also mimicking the sparse and dense configuration of the control experiment. It shows that sparse PF do not behave like AA. Sims and Hartell (2006) also made an experiment with sparse PF inputs and observed clear differences between sparse local (AA) and sparse distal (PF) synapses.

> *It is hypothesized that the association of a PF input with an AA input is similar to the association of a PF input with a CF input. However, the two are very different in terms of cellular location, with the CF input being in a position to directly interact with PF-driven inputs. Therefore, there are two major issues with this hypothesis: 1) how can subthreshold activity at one set of synapses affect another located hundreds of micrometers away on the same dendritic tree? 2) There is evidence that the CF encodes teaching/error or reward information, which is functionally meaningful as a driver of plasticity at PF synapses. The AA synapse on one set of Purkinje cells is carrying exactly the same information as the PF synapses on another set of Purkinje cells further up and down the parallel fiber beam. It is suggested that the two inputs carry sensory vs. motor information, which is why this form of plasticity was tested. However, the granule cells that lead to both the AA and PF synapses are receiving the same modalities of mossy fiber information. Therefore, one needs to presuppose different populations of granule*

> *cells for sensory and motor inputs or receptive field and contextual information. As a consequence, which granule cells lead to AA synapses and which to PF synapses will change depending on which Purkinje cell you're recording from. And that's inconsistent with there being a timing dependence of AA-PF pairing in only one direction. Overall, it would be helpful to discuss the functional implications of this form of plasticity.*

We do not hypothesise that association of the AA and PF inputs is similar to the association of PF and climbing fibre inputs. We compare them because it is the other known configuration triggering associative plasticity in Purkinje cells. It is indeed interesting to observe that even if the inputs are very small compared to the powerful climbing fibre input, they can be effective at inducing plasticity. Physiologically, the climbing fibre signal has been linked to error and reward signals, but reward signals are also encoded by granule cell inputs (Wagner et al., 2017). We have modified the discussion to make sure that we do not suggest equivalence with CF induced LTD.

Moreover, we fully agree that AA and PF synapses made up by a given granule cell carry the same information, and cannot encode sensory and motor information at the same time. AA synapses from a local granule cell deliver information about the local receptive field, but PF synapses from the same granule cell will deliver contextual information about that receptive field to distant Purkinje cells. In the context of sensorimotor learning, movement is learnt with respect to a global context, not in isolation, therefore learning a particular association must be relevant. The associative plasticity we describe here could help explain this functional association. We have clarified the discussion.

> ***Reviewer #3 (Public Review):***
>
> *Granule cells' axons bifurcate to form parallel fibers (PFs) and ascending axons (AAs). While the significance of PFs on cerebellar plasticity is widely acknowledged, the importance of AAs remains unclear. In the current paper, Conti and Auger conducted electrophysiological experiments in rat cerebellar slices and identified a new form of synaptic plasticity in the AA-Purkinje cell (PC) synapses. Upon simultaneous stimulation of AAs and PFs, AA-PC EPSCs increased, while PFs-EPSCs decreased. This suggests that synaptic responses to AAs and PFs in PCs are jointly regulated, working as an additional mechanism to integrate motor/sensory input. This finding may offer new perspectives in studying and modeling cerebellum-dependent behavior. Overall, the experiments are performed well. However, there are two weaknesses. First, the baseline of electrophysiological recordings is influenced significantly by run-down, making it difficult to interpret the data quantitatively. The amplitude of AA-EPSCs is relatively small and the run-down may mask the change. The authors should carefully reexamine the data with appropriate controls and statistics. Second, while the authors show AA-LTP depends on mGluR, NMDA receptors, and GABA-A receptors, which cell types express these receptors and how they contribute to plasticity is not clarified. The recommended experiments may help to improve the quality of the manuscript.*

As highlighted by the reviewer and developed above in response to reviewer 2, we observed a postsynaptic rundown of the EPSC amplitude. Rundown could be mistaken for a depression of synaptic currents, not for a potentiation. Moreover, we have conducted control experiments with no induction (n = 17), which give a good indication of the speed and amplitude of the rundown, and provide a baseline. Comparison shows a highly significant potentiation of the ascending axon EPSC, relative to baseline and relative to these control experiments. Depression of the parallel fibre EPSC on the other hand was not significantly different from rundown. For that reason we have not spoken of parallel fibre long term depression. The data, however, show that ascending axon and parallel fibre synapses behave very differently following the costimulation protocol.

We have discussed above in our response to reviewer 2 the potential involvement of mGluRs, NMDARs and GABAARs. We have clarified the discussion of the pathways involved in plasticity and added a diagram to highlight the links between the different molecular pathways, potential cross talk mechanisms, and the location of receptors.

> ***Recommendations for the authors:***
>
> ***Reviewer #1 (Recommendations For The Authors):***
>
> *- If Chloride concentration cannot be modified, recordings should be performed at the Chloride reversal potential to avoid strong bias in amplitude measurements (e.g. in Figures 3 and 5 outward current was observed while not visible in Figures 1 and 4.*

The balance between excitation and inhibition dictates whether there is a visible outward component, and this varies with the connections tested. Careful control experiments with SR application presented in supplementary figure 3 show that the delay of the IPSC does not significantly affect measurement of the peak amplitude of the EPSC. The reversal potential for Clin our study (-85 mV), chosen to reproduce the physiological gradient in Purkinje cells, is too low to record from Purkinje cells at this potential in good conditions as it activates the hyperpolarisation activated cation current Ih, generating huge inward currents.

> *- It is not clear whether, during the current clamp, the potential was maintained at -65 mV throughout the induction protocol.*

The potential was set and maintained around -65mV during the induction protocol. The method section has been amended to specify that point.

> *- Experiments using GABAB or endocannabinoid antagonists would have been interesting to assess the role of presynaptic plasticity occluding postsynaptic plasticity.*

We are not sure why the reviewer suggested these particular experiments to test for the role of presynaptic plasticity. GABAB and endocannabinoid receptor activation both have presynaptic effects at granule cell to Purkinje cell synapses. They decrease release probability, and as a result increase the paired pulse ratio (Dittman and Regehr, 1997; Safo and Regehr, 2005). Here we only observed a transient decrease of the paired pulse ratio. Additionally, presynaptic endocannabinoid receptor activation, linked to postsynaptic mGluR1 activation and release of endocannabinoids, was shown to be required for induction of postsynaptic PF-LTD (Safo and Regehr, 2005). This effect required climbing fibre stimulation and mGluR activation. Here we show that mGluR1 inhibition did not inhibit the PF depression nor affect the transient change in PPR. Therefore there is no indication that activation of these receptors could induce a pre-synaptic depression occluding postsynaptic plasticity.

> *- To give credit to this new plasticity in contradiction with many previous studies, induction pathways should be addressed more deeply.*

As developed earlier in response to the public review, this study does not contradict previous studies, expect maybe that by Binda et al., (2016), conducted on mice. From our point of view, our study in fact reconciles past results which have alternatively involved the mGluR or NMDAR pathways, whereas the molecular downstream pathways they recruit can easily cooperate. We aim to describe a new phenomenon and we cannot cover the mechanistic dissection which has been performed to date on plasticity in the cerebellar cortex.

> *- The quality of the figures could be enhanced by modifying the dashed line.*

We have made the dashed line more discrete.

> ***Reviewer #2 (Recommendations For The Authors):***
>
> *- Is there cross-talk between the two synaptic pathways?*

In order to explain the associative nature of AA-LTP we suggest that a signal is generated at the AA input during the induction protocol only when the PF input is also stimulated, i.e. a form of cross-talk takes place between the two synaptic territories. We have not tested for cross-talk during control conditions but we discuss the fact that given the size of the Purkinje cell dendritic tree, the size of the inputs and their geometrical configuration, it is highly unlikely. We discuss possible cross-talk mechanisms.

> *- Clarification question: "While the peak amplitude of the first response in the pair of stimulations showed a progressive decline, the peak amplitude of the second response of both AA and PF underwent either LTP or LTD respectively..." Does this mean that all LTP/LTD figures show the amplitude of the second EPSC in the paired pulse stimulation, and that the first EPSC has a different response? If so, this should be mentioned in the Methods section and implications discussed.*

All figures show both the amplitude of the first and second EPSCs in the pair of stimulations. In Figure 1A, 3A, 4A and 5B the paired stimulation protocol is depicted with colours and symbols used in the associated graphs, with closed symbols for the first and open symbols for the second EPSC. Figure legends have been amended to clarify this point. The average values given in the Results section and figure legends relate to the first EPSC only for clarity. As can be seen from the figures, long term plasticity affected the first and second EPSC in a very similar manner. However, individual symbols show that during a transient period, the first and second EPSCs are differentially affected by the induction protocol, resulting in a transient change of the PPR.

> *Minor suggestions:*
>
> *- It would be helpful to have a reference for the statement that 1-2% of stimulated fibers come from nearby GCs when stimulation is distal.*

We have modified the text to explain our calculation based on the data of Pichitpornchai et al., 1994. P4 result section.

> *- Does the shading over the plasticity time course traces come from the standard error of the mean?*

Shading over the plasticity time course plots shows the standard error of the mean. This is now clearly stated in figure legends.

> ***Reviewer #3 (Recommendations For The Authors):***
>
> *Major points:*
>
> *(1) Whether the plasticity between AAs and PCs is regulated by the post-synaptic or pre-synaptic mechanisms should be addressed or discussed. Based on the results of PPR (mostly unchanged after induction), the post-synaptic mechanism may be more significant. Supplemental Figure 2C shows a trend toward a positive correlation between AALTP and the number of spikes, suggesting intracellular calcium levels in the post-synaptic Purkinje cells may be important. Whether this is true or not can be directly tested by the addition of BAPTA in the recording pipettes.*

The absence of a long lasting effect on the paired pulse ratio (PPR) indicates that postsynaptic mechanisms are involved in long term changes. This is in line with the dependence of plasticity induced with similar protocols on the concentrations of NO and postsynaptic calcium, both affecting postsynaptic targets, as developed in our response to reviewer 2. BAPTA interferes with calcium and mGluR signalling, and could be used to further confirm the involvement of a postsynaptic mechanism, however, we did not wish to pursue further the dissection of the signalling cascade. We have modified the Results and Discussion sections to include a discussion of pre and postsynaptic mechanisms.

> *(2) Most results from the plasticity experiments are shown as average/sem and do not include individual data, making ithard to appreciate the magnitude of the changes. The authors could show the individual data at some time points (e.g. 5 min before and 30 min after induction), plot bar-graphs (Figure 2C with individual data), or boxplots to compare different conditions and perform statistics.*

Individual data points are now visible for plasticity induction in Figure 2C and Supplementary Figure 2 for a number of conditions. Statistics have been performed as detailed in the text and legend of Fig 2.

> *(3) In addressing point #2, it is strongly recommended that the authors include the values for controls without inductionbecause AA/PF-EPSCs undergo significant run-down. In most experiments, the authors compare the magnitude of plasticity with baseline changes in Supplemental Figure 1. This should not be appropriate for some experiments, such as Figures 3 & 4, where pharmacological treatments are performed. The authors should carefully consider including the appropriate controls from baseline recording to rule out significant confound by the run-down.*

We agree that control experiments without stimulation (no Stim) are only appropriate controls for the initial synchronous stimulation and AA and PF only experiments (Fig 1). All the other experiments were compared to the synchronous stimulation experiments, not to control No Stim. The synchronous stimulation protocol is strictly the same as that applied in experiments with pharmacological treatments and the appropriate control to test whether treatments affected plasticity. This is now systematically specified in the Results section.

> *(4) The authors recorded mixed EPSC/IPSCs and used a fitting approach to extract EPSCs. Applying AMPA-receptor blockers to check that extracted IPSCs are correctly predicted may solidify the reliability of the approach. An additional concern is that this approach can only be used if the waveform of EPSC/IPSC does not change with plasticity. The authors should compare the waveforms between conditions to address this point.*

Fits were not used to extract EPSCs. EPSCs were isolated by blocking IPSCs with SR95531, and the IPSCs were then extracted by subtraction from the mixed EPSC/IPSC. Fits were then done of the isolated EPSC and the extracted IPSC. This procedure was applied both at the start of the experiment and at the end to avoid changes in kinetics that would influence measurements. A section of supplementary material is devoted to this analysis. Isolating IPSCs using AMPAR blockers is not possible as IPSCs are disynaptic. AMPAR blockers would fully suppress inhibition.

> *(5) While the AA-LTP depends on NMDA-Rs, which cell type is responsible is not clear. Recording NMDA components in AA/PF-EPSCs should be informative in addressing this point. Cesana et al suggested that AA induces significant activation of NMDA-Rs in Golgi cells (PMID: 23884948). Whether AA stimuli could significantly evoke NMDA current in the experimental condition used in this paper could provide essential information.*

The granule cell to Purkinje cell EPSCs are devoid of an NMDAR component (Llano et al., 1991), and there is no postsynaptic NMDARs at granule cell to PC synapses, but a proportion of presynaptic boutons show the presence of NMDARs (Bidoret et al, 2009). This is now stated clearly on p8. Presynaptic NMDAR have been involved in LTP and LTD of parallel fibre synapses (Casado et al., 2002; Bouvier et al., 2016; Schonewille et al., 2021), and linked to the activation of NOS in granule cell axons. However, we do not know whether presynaptic NMDARs are also present at AA synapses. NMDAR and NOS are also expressed by molecular layer interneurons, and have sometimes been involved in LTD induction (Kono et al., 2019), although this is disputed. In the paper by Cesana (2013), white matter stimulation activated mossy fibre inputs to granule cells, and as a consequence, granule cell to Golgi cell disynaptic EPSCs. The authors identified AA synapses on the basolateral dendrites of Golgi cells, and showed NMDAR activation associated with the mossy fibre to granule cell EPSC. Granule cell to Golgi cell synapses were shown to activate both postsynaptic AMPA and NMDA receptors (Dieudonné, 1999). But to our knowledge, Golgi cells do not express NOS. Therefore it is unlikely that activation of NMDARs in Golgi cells is linked to synaptic plasticity in Purkinje cells.

> *(6) Pharmacological experiments in Figure 3 show that AA-LTP is dependent on mGluR. The authors mentioned that it could be explained by the presence and absence of mGluRs in PFs and AAs, respectively. This is an important and reasonable possibility and should be tested. The authors could simply check whether slow EPSCs can be recorded by the AA activation.*

Activation of the mGluR slow EPSC by AA stimulation would reveal the presence of mGluRs at AA inputs. We know, however, that sparse PF stimulation does not activate the mGluR slow EPSC nor endocannabinoid release unless glutamate transporters are blocked (Marcaggi and Attwell., 2005). This is thought to reflect insufficient glutamate buildup in the sparse configuration to activate mGluR1s. AA inputs are sparsely distributed and are not expected to activate the slow EPSC either, and this is confirmed by our own experiments (CA personal communication). However, mGluR1 mediated Ca2+ release from stores shows a higher sensitivity to glutamate than the slow EPSC (Canepari and Ogden, 2006) and might take place with sparse inputs, but Ca2+ signals have not been investigated in this configuration. Therefore the absence of the slow EPSC is not sufficient proof that mGluR1s are not activated and not present at AA synapses. This is now further discussed p12.

> *Minor points:*
>
> *(1) The authors should describe how they adjusted the stimulation strength for both AAs and PFs.*

Adjustment of the stimulation intensity is now described in the Methods section.

> *(2) A rationale explaining why the authors chose the current induction protocol (synchronous stimulation of both inputs) should be included. This will help the readers to understand the background of the study.*

Papers by Sims and Hartell (2005, 2006) and experimental evidence indicated that AA and PF inputs may have different properties, and as a result may play different roles. Moreover, based on the morphology of the cerebellar granule cell and Purkinje cell, AA and PF inputs can carry different information to a given Purkinje cell. We reasoned that co-presentation of the inputs might represent an important piece of information for the circuit, signalling functional association, and lead to plasticity, as seen for motor command and sensory feedback in cerebellar-like structures, or for PF and climbing fibre. We have tried to convey that rational in the abstract and introduction.

> *(3) Supplemental Figure 2B: the x-axis may be labeled incorrectly, Is the x-axis of the top graph for PF PF-EPSC? Thex-axis for the bottom graphs should be the summation of AA- and PF-EPSCs.*

This has been corrected.

> *(4) "mglur1" on page 10 should be mGluR1.*

This has been corrected.

https://doi.org/10.7554/eLife.96140.2.sa0